



Cite this: *J. Mater. Chem. B*, 2022, 10, 7239

## Hemostatic biomaterials to halt non-compressible hemorrhage

Shuaibing Jiang,<sup>a</sup> Shiyu Liu,<sup>b</sup> Sum Lau<sup>b</sup> and Jianyu Li<sup>\*acd</sup>

Non-compressible hemorrhage is an unmet clinical challenge, which occurs in inaccessible sites in the body where compression cannot be applied to stop bleeding. Current treatments reliant on blood transfusion are limited in efficacy and complicated by blood supply (short shelf-life and high cost), immunogenicity and contamination risks. Alternative strategies based on hemostatic biomaterials exert biochemical and/or mechanical cues to halt hemorrhage. The biochemical hemostats are built upon native coagulation cascades, while the mechanical hemostats use mechanical efforts to stop bleeding. This review covers the design principles and applications of such hemostatic biomaterials, following an overview of coagulation mechanisms and clot mechanics. We present how biochemical strategies modulate coagulation and fibrinolysis, and also mechanical mechanisms such as absorption, agglutination, and adhesion to achieve hemostasis. We also outline the challenges and immediate opportunities to provide comprehensive guidelines for the rational design of hemostatic biomaterials.

Received 15th March 2022,  
Accepted 13th May 2022

DOI: 10.1039/d2tb00546h

rsc.li/materials-b

### 1. Introduction

Significant mortality is associated with hemorrhage, arising from trauma, surgery and coagulopathy.<sup>1</sup> This condition causes 43% and 90% of deaths following traumatic injury in the civilian and military setting, respectively.<sup>2,3</sup> To stop bleeding,

the human body forms blood clots at the bleeding sites. This process of hemostasis is often slow and ineffective under severe bleeding conditions like hemorrhage. These issues are critical given the short time window for hemostatic management, known as “platinum 5 minutes”, and pressurized blood flows under hemorrhage resulting from penetrating trauma.<sup>4</sup>

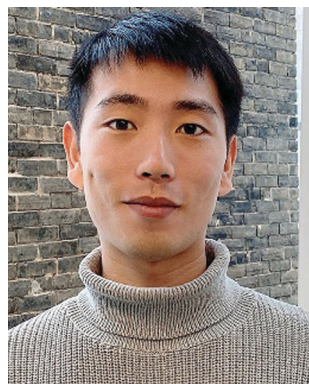
When blood loss occurs in the torso and other body parts where direct compression cannot be applied to stop the bleeding, it is noncompressible hemorrhage that remains an unmet clinical challenge. For non-compressible hemorrhage, transfusion of whole blood or blood components is the current “gold

<sup>a</sup> Department of Mechanical Engineering, McGill University, Montreal, Quebec, Canada. E-mail: jianyu.li@mcgill.ca

<sup>b</sup> Faculty of Engineering, The University of Hong Kong, Hong Kong, China

<sup>c</sup> Department of Biomedical Engineering, McGill University, Montreal, Quebec, Canada

<sup>d</sup> Department of Surgery, McGill University, Montreal, Quebec, Canada



Shuaibing Jiang

Shuaibing Jiang is currently a PhD candidate in the Department of Mechanical Engineering at McGill University, Canada. He received his MS degree in chemistry from Soochow University, China, and BS degree in applied chemistry from Northeastern University, China. His research interests include hemostatic biomaterials, bioadhesives, and living materials for biomedical applications.



Shiyu Liu

Shiyu Liu is a doctoral student in the Department of Mechanical Engineering at McGill University, Canada. He received a Bachelor of Engineering degree in Engineering Mechanics and a Master of Engineering degree in Mechanics from Xi'an Jiaotong University in China. His scientific interest is biomechanics and biomaterials, and his research focuses on experimental and computational mechanics for blood clot fracture and the development of hemostatic materials.



**Fig. 1** Schematics of bleeding and hemostasis. (a) Bleeding at an injury site. Hemostatic technologies based on (b) biochemical mechanisms and (c) mechanical mechanisms.

standard". However, blood and its components derived from donors are usually accompanied by limited availability, contamination risks, immunogenicity, short shelf-life, high cost, and batch-to-batch variation. To address these issues, extensive efforts have been made in developing hemostatic biomaterials, the focus of this review.

Attempts to expedite and promote hemostasis have led to a variety of hemostatic technologies for managing bleeding complications.<sup>5–9</sup> Some have been translated into clinically used products, saving lives in operating rooms and on battlefields. Typically, these hemostatic biomaterials are applied by intravenous or intracavitary administration to manage the non-compressible hemorrhage. Ideal hemostatic biomaterials could mimic, amplify, and leverage hemostatic mechanisms. They should also be biocompatible, biodegradable, and bioactive to promote tissue regeneration.<sup>10,11</sup> Other translational

considerations include storage stability, ease of implementation, and cost effectiveness. The existing hemostatic materials can hardly meet all the above requirements and thus call for further development.

To guide the rational design of new hemostatic biomaterials, this review will start with an overview of coagulation mechanisms and mechanics of blood clots. According to the underlying mechanisms, we will categorize the existing materials into two categories: biochemical hemostats and mechanical hemostats (Fig. 1); note that some materials fit into both. The former centers on native coagulation cascades, while the latter exerts mechanical efforts to stop bleeding. The designs and applications of the two hemostats will be described and critically discussed. This review will conclude with the remaining challenges in the field, as well as immediate opportunities for next-generation hemostatic biomaterials.



**Sum Lau**

*Sum Lau is an engineering science undergraduate student from the University of Hong Kong, Hong Kong, China, double majoring in biomedical engineering and materials engineering. He joined Dr Jianyu Li's Laboratory at McGill University, Montreal, Canada, from May to August 2021 through a Mitacs Globalink Research Internship, where he studied and performed modelling on blood clot contraction, as well as evaluated blood clots as a novel actuator*

*with hemostatic properties. Apart from blood mechanics or biomechanics in general, he is also interested in single cell analysis, genetic engineering, biosensing, biomaterials, and medical robotics.*



**Jianyu Li**

*Dr Jianyu Li is a Canada Research Chair and Assistant Professor in the Departments of Mechanical Engineering and Biomedical Engineering at McGill University. He graduated from Zhejiang University and obtained a PhD degree in Mechanical Engineering from Harvard University. He conducted postdoctoral research on biomaterials at the Harvard Wyss Institute. His current research is focused on the design and mechanics of biomaterials such as*

*hydrogels and tissue adhesives and their applications in tissue repair and regeneration.*

## 2. Coagulation and clot mechanics

### 2.1 Blood coagulation

Blood coagulation provides the basis for hemostatic technologies. The endothelium of healthy blood vessels serves as a barrier to prevent blood clotting by avoiding the adsorption of coagulation-relevant proteins, and secreting a variety of bioactive molecules including heparin-like molecules, thrombomodulin, nitric oxide, and prostacyclin.<sup>12</sup> When the endothelium is injured, blood coagulation proceeds with a series of coagulation cascades in relation with the components and tissue microenvironment of blood (Fig. 2). The key contributors are platelets and fibrinogen, which are instrumental to the primary and secondary hemostasis, respectively.

For the primary hemostasis (Fig. 2a), injuries expose the subendothelial collagen, where the von Willebrand factor (vWF) secreted by endothelial cells inherently resides (subendothelial vWF), and the plasma vWF circulating in blood is deposited subsequently.<sup>13</sup> The exposed collagen and immobilized vWF further interact with platelets *via* platelet membrane receptors (*e.g.*, glycoprotein Ia/IIa (GP Ia/IIa) and GP VI for collagen

binding, and GP Ib for vWF), leading to platelet adherence at injury sites.<sup>13,14</sup> Upon being arrested and activated, they release granule contents such as adenosine diphosphate (ADP), thromboxane A<sub>2</sub> (TxA<sub>2</sub>), vWF and thrombin, which further amplify platelet activation.<sup>15</sup> A series of signaling events result in the shape change of platelets and activation of GP IIb/IIIa, an integrin receptor present at high density on the platelet surface. Fibrinogen bridges adjacent GP IIb/IIIa molecules and aggregates platelets. These mechanisms of primary hemostasis lead to the formation and adherence of platelet plugs at the bleeding sites.

To strengthen the platelet plug, the secondary hemostasis takes effect to form a fibrin network within blood clots (Fig. 2b).<sup>16,17</sup> Such coagulation cascades are divided into the extrinsic pathway and the intrinsic pathway at the initial stage. Following injuries, the extrinsic pathway is triggered by exposed tissue factors (TF) expressed on subendothelial cells, which bind to coagulation factor VII (FVII) and activate factor X (FX) to yield moderate amounts of thrombin (FIIa). The generated thrombin further activates other coagulation factors part of the intrinsic pathway. Also, the intrinsic pathway can be triggered



**Fig. 2** Mechanisms of primary and secondary hemostasis, fibrinolysis, and hemostatic targets derived from coagulation cascades. (a) Injuries expose the subendothelial collagen and von Willebrand factor (vWF), as well as tissue factor (TF) bearing cells at the wound sites. Platelets adhere to the bleeding sites through collagen and vWF, then undergo activation and aggregation *via* fibrinogen-mediated bridging, and eventually form a platelet plug (primary hemostasis). (b) The intrinsic pathway is activated when blood contacts negatively charged surfaces. The exposed TF triggers the extrinsic coagulation pathway and generates thrombin (IIa). Two pathways converge into a common pathway where the prothrombinase complex (FVa + FXa + FII) is formed on the platelet surface, further promoting the production of thrombin for converting fibrinogen into fibrin. Fibrin polymerizes and assembles into a fibrous network that is crosslinked by FXIII (secondary hemostasis). (c) Fibrin is subject to fibrinolysis, leading to the degradation of blood clots. (d) Hemostatic targets, including platelets (either natural or synthetic), coagulation factors (*e.g.*, I, II, VII, and XIII), and antifibrinolytics (*e.g.*, tranexamic acid), steer the development of hemostatic biomaterials. (a and b) are adapted with permission from ref. 11. Copyright 2021, Springer Nature.

by negatively charged molecules/polymers and surfaces such as the high-molecular-weight kininogen (HMWK) on the subendothelial collagen. Through the cascade reactions of coagulation factors, both pathways converge to form the prothrombinase complex (FVa + FXa + FII) on the platelet surface in the presence of calcium, which further enables the amplified generation of thrombin capable of converting fibrinogen to fibrin. Fibrin can self-assemble into fibers and form a fibrous network cross-linked by the coagulation factor XIII (FXIII). The fibrin is subject to fibrinolysis, leading to the clearance of blood clots (Fig. 2c). Altogether, the primary and secondary hemostasis yields blood clots at the bleeding sites.

The clotting duration required to form solid clots out of liquid blood is critical for hemostasis. Faster clotting is prone to shorten the bleeding duration and the amount of blood loss. The clotting duration depends on not only the native coagulation cascades (varies pathologically), but also exogenous factors that intervene in the coagulation process. A variety of assays are applied to measure the clotting time. In clinics, prothrombin time (PT) and activated partial thromboplastin time (aPTT) are measured with plasma, while the activated clotting time (ACT) test is performed on the whole blood. These are widely used to analyze the functions of coagulation factors and anticoagulants. Simple tests like vial inversion can be used to roughly determine the clotting time. Thromboelastography (TEG) and rheology measurements are much more quantitative to monitor the whole kinetics of the clotting process. Also, the TEG can generate parameters that reflect clot strength and fibrinolysis, while the rheometer can output the shear modulus-time profiles. Due to the complexity of the coagulation cascade and its sensitivity to testing conditions, a range of clotting durations is reported in the literature. For TEG assay without addition of activators, a clotting time of the whole blood of humans is reported as 630 seconds.<sup>18</sup> According to rheological measurements, normal whole blood clotting generally reaches the gel point within 240 seconds, which can be shortened to 10 seconds with the administration of thrombin;<sup>18,19</sup> extreme cases such as severe hemophilia even lead to no clotting.

## 2.2 Blood clot mechanics

The coagulation cascades yield blood clots, serving as plugs to stop bleeding and seal the injury sites. This purpose of hemostasis is mechanical in nature. The mechanics of blood clots are essential to the hemostatic function, as well as the downstream consequences such as wound healing and tissue regeneration. Clot mechanics studied by TEG indicates that decreased clot stiffness is associated with bleeding disorders in some patients who have hemophilia and von Willebrand disease.<sup>20</sup> Despite the appreciation of clot mechanics on hemostasis, the exact link demonstrated *in vivo* is missing. The gap was filled recently with a rodent study, showing that both adhesive and cohesive failures of blood clots lead to rebleeding and decrease survival from hemorrhage *in vivo*.<sup>21</sup> Substantiating the direct link between clot mechanics and hemostasis requires further investigation.

The mechanical properties of blood clots include stiffness (*i.e.*, elastic modulus or shear modulus), strength, viscoelasticity,

Table 1 Mechanical properties of blood clots

Properties	Value	Note
Elastic modulus <sup>22</sup>	10 kPa	Bovine whole blood
Shear modulus <sup>23</sup>	5 kPa	Bovine whole blood
Strength <sup>24</sup>	2.20 ± 0.25 kPa	Human platelet-rich plasma
Fracture toughness <sup>25</sup>	5.90 ± 1.18 J m <sup>-2</sup>	Human whole blood
Permeability <sup>26</sup>	4.4 × 10 <sup>-9</sup> cm <sup>2</sup>	Bovine whole blood

poroelasticity, and fracture toughness.<sup>22-26</sup> The representative value for each property is summarized and listed in Table 1; some of the testing methods and apparatus have been reviewed elsewhere.<sup>20,27</sup> Attention is called to the difference between toughness and fracture toughness; toughness quantifies the energy dissipation capacity of an unnotched sample in a unit of J m<sup>-3</sup>, while the fracture toughness in a unit of J m<sup>-2</sup> reflects the resistance against crack propagation.<sup>28</sup> It should be noted that the list is by no means exhaustive.

As can be seen from the above table, blood clots are mechanically inferior to other biological materials such as blood vessels and skin. Considering fracture resistance, the fracture toughness of blood clots is measured at ~1 J m<sup>-2</sup>, which is two and three orders of magnitude lower than that of blood vessels and skin, respectively. The mechanical mismatch is concerning as the clot can neither survive the force from the surrounding tissues, nor restore the biomechanics of the injured tissues. A downstream consequence is the mechanical failure of clots, causing rebleeding and hemorrhage. This issue necessitates strategies to augment the clot mechanics, one of the main focuses of the existing invention technologies.

## 2.3 Hemostatic mechanisms

The overarching goal of hemostatic technologies is to form, accelerate, and/or strengthen blood clots. The hemostatic targets, including platelets (natural or synthetic), coagulation factors (*e.g.*, I, II, VII, and XIII), and antifibrinolytics (*e.g.*, tranexamic acid), steer the development of hemostatic biomaterials (Fig. 2d). To achieve such goals, a variety of strategies have been developed and can be divided into two main categories: biochemical and mechanical approaches.

The biochemical approaches leverage biochemical cues to intervene in two biochemical processes underpinning hemostatic applications: hemostasis and fibrinolysis. As described above, hemostasis is a synergy of platelet plug formation (primary hemostasis) and fibrin network generation (secondary hemostasis) at the bleeding sites. Accordingly, biochemical hemostatic materials can target the two processes. There are strategies aimed at leveraging and mimicking the adhesion, activation, and aggregation properties of platelets to promote hemostasis. The other is manipulating various coagulation factors (*e.g.*, fibrin, thrombin, FVIII, and FXIII) to modulate the initiation, propagation or stabilization of the fibrin network, thereby enhancing the hemostatic performance. In addition, a different hemostatic approach is associated with the fibrinolytic system. In physiological settings, there is a highly regulated balance between clot formation and clot lysis. Fibrinolysis plays

an important role in regulating blood clot formation and lysing the clot during wound healing.<sup>29</sup> Therefore, the antifibrinolytic mechanism can be utilized for an enhanced outcome of hemostasis.

In contrast to the biochemistry focus of biochemical hemostats, the mechanical approaches exert primarily mechanical effects to stop bleeding. The mechanical efforts exerted by mechanical hemostats include blood absorption, agglutination and bio-adhesion. Consequently, physical barriers are formed at the bleeding sites to stop the blood flow. The key to these approaches is only passively interacting with blood by mechanical forces to impart complete/partial hemostasis. Because of this feature, the mechanical mechanism is advantageous for being independent of native coagulation cascades and blood disorders, ensuring wide applicability and compatibility with the biochemical strategies. To further showcase the two kinds of hemostats, we elaborate their design strategies and applications as follows.

### 3. Biochemical hemostatic biomaterials

A variety of biochemical cues have been explored to mediate blood clotting for hemostatic applications. Examples include platelet, thrombin, fibrin and other coagulation factors derived from human plasma or synthesized *via* recombinant DNA technology. In addition to the coagulation cascades, fibrinolysis is another target pathway, which can be retarded with antifibrinolytic agents to extend the stability of blood clots. A summary of biochemical hemostatic biomaterials in terms of their formulation, hemostatic mechanism, efficacy, application scenarios and advantages and disadvantages is shown in Table 2. More details about biochemical hemostats are presented as follows.

#### 3.1 Platelet-based hemostats

Platelets are a key player in stanching bleeding at the injury sites. As noted in Section 2.1, the platelets fulfill their hemostatic function by forming platelet plugs. Transfusion of platelets has been increasingly used during the past few decades.<sup>30,31</sup> Despite the efficacy shown in the clinic, this strategy is complicated by the shortage, shelf-life (3–5 days) and batch-to-batch variations of donor-derived platelets, contamination risks, and immunologic reactions. To address the supply issue, *in vitro* production of platelets from progenitor or stem cells has been explored,<sup>32</sup> but the mass production of high-quality and cost-effective platelets remains a distant prospect.

Alternative strategies are used to develop artificial platelets or platelet-mimicking components. They are manufactured into a particulate form or polymer solution, and can be administered intravenously before or immediately following injuries for the prophylactic management of coagulopathy and acute hemorrhage control, respectively. The artificial platelets can mimic the native counterparts in terms of adhesion, aggregation and contraction.

The adhesion and aggregation of platelets are mediated by the interactions between platelet surface receptors (GPIb $\alpha$ , GPIa-IIa and GPIIb-IIIa) and platelet-binding components (*e.g.*, vWF, collagen and fibrinogen) as discussed above. Targeting the adhesion of platelets, the surface of liposomes is decorated with recombinant platelet glycoproteins GPIb $\alpha$  and GPIa-IIa.<sup>33</sup> These synthetic particles bind effectively to collagen and vWF-coated surfaces under high shear flow conditions. To mimic the aggregation properties of platelets, fibrinogen has been used to coat particles or cells. As an example, fibrinogen-coated RBCs are shown to induce platelet aggregation *in vitro* and decrease the bleeding time in thrombocytopenic rats *in vivo*.<sup>34</sup> Another system called Synthocytes is albumin microspheres coated by fibrinogen,<sup>35</sup> such particles enable the aggregation of activated platelets *in vitro* and reduction of bleeding time in a rabbit ear-punch model.

To mimic the platelet function, researchers also developed artificial platelets carrying synthetic peptides, instead of proteins, because the peptides possess higher stability, lower immunogenicity and batch-to-batch variations, compared to proteins. As GPIIb-IIIa binds to fibrinogen through an RGDS tetrapeptide (Arg-Gly-Asp-Ser), the RGD sequence was conjugated to the RBC surface,<sup>36</sup> yielding modified RBCs that can co-aggregate with activated platelets and bind to platelets adherent to collagen. Another similar example is RGD-functionalized polymeric nanoparticles developed for the use of intravenous hemostats.<sup>37</sup> Since the RGD peptide has ubiquitous interactions with cells and the extracellular matrix,<sup>38</sup> it may pose thrombogenic risks and impart crosstalk with other cellular processes. An alternative peptide is H12 (His-Leu-Gly-Gly-Ala-Lys-Gln-Ala-Gly-Asp-Val), which mediates GPIIb-IIIa/fibrinogen binding. Liposomes and albumin particles decorated H12 are shown to enhance platelet aggregation and shorten the bleeding time by 50% in both ear punch models of thrombocytopenic rabbits and rats.<sup>39,40</sup> Incorporation of more than one peptide has also been explored, as exemplified with SynthoPlate, a liposomal vesicle carrying pro-adhesive and pro-aggregatory motifs simultaneously.<sup>41</sup> The vWF-binding peptide (VBP), collagen-binding peptide (CBP), and fibrinogen-mimetic peptide (FMP) were firstly conjugated to an amphiphilic polymer (Fig. 3a). The resulting conjugates further form liposomal vesicles of 200 nm diameter. Following intravenous administration, SynthoPlate is co-localized with platelets at the injury sites. These artificial platelets demonstrate promising efficacy in reducing blood loss, stabilizing blood pressure, and improving survival in small and large animal models with trauma and thrombocytopenia.

Another function of platelets is contracting the clot *via* their actin-myosin machinery. This attribute leads to volumetric reduction and concomitant stiffening of blood clots in the injury sites.<sup>27</sup> The resulting benefits include strengthening the clot, approximating wound edges and restoring blood flow by decreasing the obstructive clots.<sup>42</sup> Inspired by this, a platelet-like microgel system was developed by decorating deformable microgels with a specific fibrin-binding nanobody obtained from phage-display biopanning (Fig. 3b).<sup>43</sup> These platelet-like particles (PLPs) actively bind to and collapse the fibrin network,

Table 2 Summary of biochemical hemostatic biomaterials

Hemostatic biomaterials	Hemostatic mechanism	Hemostatic efficacy	Application scenarios	Advantages and disadvantages
Fibrinogen-coated RBCs <sup>34</sup>	Platelet-mimicking aggregation	Decrease tail bleeding time from 18 min to 4.5 min in autoimmune thrombocytopenic rats	Intravenous administration for autoimmune thrombocytopenia	Autologous RBCs facilitate hemostasis; use of toxic formaldehyde to bind fibrinogen
RGD functionalized polymeric nanoparticles (PLGA-PLL-PEG) <sup>37</sup>	Platelet-mimicking adhesion	Decrease bleeding time from 240 s to 131 s in a rat femoral artery injury model	Intravenous administration for trauma	Good performance; thrombogenic risks and crosstalk with other cellular processes
Liposomes and albumin particles decorated with the H12 peptide <sup>39,40</sup>	Platelet-mimicking aggregation	Shorten bleeding time by 50% in both ear punch models of thrombocytopenic rabbits and rats	Intravenous administration for thrombocytopenia	Specific binding with fibrinogen to enhance platelet aggregation; hemostatic efficacy is dependent on platelets
Liposomal vesicles carrying the vWF-binding peptide (VBP), collagen-binding peptide (CBP), and fibrinogen-mimetic peptide (FMP) <sup>41</sup>	Platelet-mimicking adhesion and aggregation	Reduced blood loss by ~50% and significantly improved survival (100% versus 25% in the first hour, 75% versus 0% at the end of 2 hours) in the pig femoral artery hemorrhage model	Intravenous administration for traumatic non-compressible hemorrhage	Injury site-selective adhesion and aggregation mechanisms, proved hemostatic efficacy in large animal models; administration time window not studied
Ultra-low crosslinked microgels (pNIPAm-AAc) decorated with fibrin-binding nanobodies <sup>43</sup>	Platelet-mimicking adhesion and contraction	Shorten bleeding time from around 140 s to 120 s and decrease blood loss from around 1.4 g to 1.1 g in a rat femoral vein injury model	Intravenous administration for trauma	Comparable hemostatic efficacy with FVIIa, ability to induce clot contraction but require a much longer timescale
Polymer (HA) modified with the vWF-binding peptide (VBP) and collagen-binding peptide (CBP) <sup>44</sup>	Platelet-mimicking adhesion	>97% reduction in both bleeding time and blood loss in a mouse tail vein laceration model, survival time improved by 284% in a rat inferior vena cava traumatic model	Intravenous administration for point-of-care treatment of noncompressible hemorrhage	Storable and easily administered; hemostatic efficacy relies on platelets at the injury site
Self-propelled microparticles of calcium carbonate (CaCO <sub>3</sub> ) formulated with thrombin and tranexamic acid (TXA) <sup>52</sup>	Thrombin	Bleeding stopped in 78% of mice in 10 minutes	Intravenous administration for external or intraoperative bleeding	Far-reaching applications for the delivery of hemostatic therapeutics
Self-propelling Janus particles MSS@CaCO <sub>3</sub> loaded with thrombin <sup>53</sup>	Thrombin	Hemorrhage in rabbit liver and femoral artery models is controlled in ~50 s and ~3 min, respectively	Local administration for the control of perforating and irregular hemorrhage	Directional transport into the hemorrhage sites, rapid clotting
Snake extract-laden hemostatic hydrogel (GelMA) <sup>55</sup>	Thrombin analogue	Fast hemostasis (~45 s and ~34 s) and reduced blood loss by 79% and 78% in liver incision and rat tail models, respectively	Local administration noncompressible bleeding	Excellent functions of blood resistance, adhesive properties, fast blood clotting
Tissue-factor-targeted peptide amphiphile nanofibers <sup>63</sup>	FVII-mimicking	Decreased blood loss in comparison to sham and backbone nanofiber controls by 35–59%	Intravenous administration for noncompressible torso hemorrhage	Injectable nanotherapeutics can localize selectively to the hemorrhage sites
Synthetic polymer (PolySTAT) carrying a specific fibrin-binding peptide <sup>45</sup>	FXIII-mimicking	100% survival in a rat trauma-induced coagulopathy (TIC) model, requiring only 42% of the maximum allowed in-fusion volume	Intravenous administration for the management of congenital and acquired bleeding disorders	Circulating innocuously in the blood, enhancing clot resistance to enzymatic degradation
Tranexamic acid (TXA)-loaded trauma-targeted nanovesicles (T-tNVs) <sup>72</sup>	Antifibrinolytic agent	Blood loss rates (%TBV/min) for saline-treated and T-tNV-treated rats were 4.9% min <sup>-1</sup> and 0.7% min <sup>-1</sup> , respectively	Intravenous administration for trauma-associated hemorrhage and coagulopathy	Enhancing the systemic safety and injury site-localized efficacy of TXA in trauma treatment applications
Tranexamic acid (TXA)-loaded microparticles of gelatin <sup>76</sup>	Antifibrinolytic agent	Hemostasis time reduced to <2 minutes, shorter than normal clotting (~8 min)	Local administration for internal bleeding	Blood absorption, rapid hemostasis, and safe use in internal applications

resulting in clot contraction over a much longer timescale (tens of hours) compared to that by platelets (a few hours). The possible mechanisms are accumulated local deformation of the fibrin network *via* multivalent microgel–fibrin binding and an uneven distribution of tension in the network. PLPs are shown to augment clotting *in vitro* under physiological flow conditions. Also, they can home in on the injury sites, decrease the bleeding

time, and reduce blood loss comparable to that by administration of FVIIa in a rat femoral vein injury model.

In addition to the particle shape, platelet-mimicking systems can be polymeric for higher solubility, flexibility, and multivalent affinity toward their targeted moieties.<sup>44,45</sup> As an example shown in Fig. 3c, an injectable polymer hemostat named HAPPI consists of hyaluronic acid (HA) modified with the VBP and CBP, capable

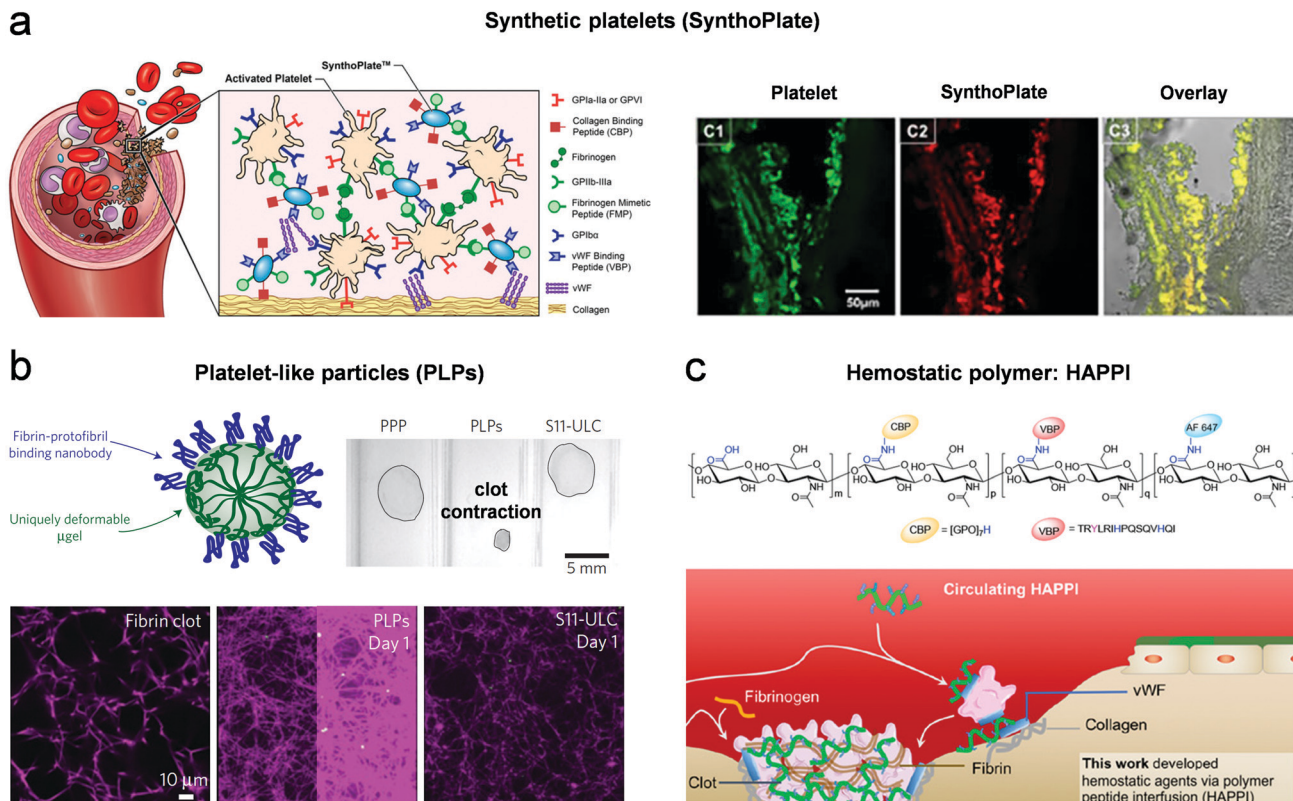


**Fig. 3** Platelet-based hemostats. (a) SynthoPlate is the liposomal vesicle decorated with pro-adhesion peptides (vWF-binding peptide VBP and collagen-binding peptide CBP) and a pro-aggregation peptide (fibrinogen-mimetic peptide FMP). It can specifically adhere to the injury sites and integrate with platelets.<sup>41</sup> Reproduced under the terms of the CC BY Creative Commons Attribution 4.0 International License. Copyright 2018, The Authors, published by Springer Nature. (b) Platelet-like particles (PLPs) can bind and collapse the fibrin network.<sup>43</sup> Reproduced with permission. Copyright 2014, Macmillan Publishers. (c) HAPPI is composed of hyaluronic acid (HA) modified with the VBP and CBP, which selectively binds to subendothelial collagen and activated platelets.<sup>44</sup> Reproduced under the terms of the CC BY-NC Creative Commons Attribution 4.0 NonCommercial License. Copyright 2020, The Authors, published by American Association for the Advancement of Science.

of selectively binding to the subendothelial matrix and activated platelets.<sup>44</sup> Instead of forming a physical plug by itself, HAPPI facilitates the recruitment and aggregation of platelets at the injury site, thereby enhancing blood clotting. It has been demonstrated to be storable, easily administrated, safe and efficient in improving the survival time of noncompressible hemorrhage. Although it is promising for point-of-care treatment, the dependence on natural platelets limits its applications for patients with deficiency or dysfunction of platelets.

### 3.2 Thrombin and fibrin-based hemostats

Thrombin and fibrin are key components for fibrin network formation. Thrombin cleaves fibrinopeptides from fibrinogen, resulting in a fibrin monomer. Fibrin self-assembles into two-stranded protofibrils *via* the non-covalent knob-hole interactions, which further aggregate laterally and longitudinally to form fibers and the branched network.<sup>46–48</sup> Accordingly, the transfusion of fibrinogen concentrates or prothrombin complex concentrates has been extensively developed for managing severe bleeding.<sup>49,50</sup> For example, the fibrinogen concentrate derived from human plasma is currently manufactured as four products: Haemocomplettan (CSL Behring), Clottafact (LFB),

Fibrinogen HT (Benesis), and FibroRAAS (Shanghai RAAS).<sup>51</sup> Also, the prothrombin complex concentrates are recommended in preference to other treatments and have been the current clinical mainstay.<sup>50</sup>

Compared to systemic transfusion, the topical delivery of thrombin deep into damaged tissues is believed to stop uncontrolled bleeding quickly. However, it is difficult to transport the hemostatic agents into deep and complex bleeding sites against pressurized blood flows. Therefore, as shown in Fig. 4a, a self-propelled particle system by gas-generation was developed.<sup>52</sup> Composed of calcium carbonate ( $\text{CaCO}_3$ ) mixed with a solid organic acid, the particles rapidly produce carbon dioxide ( $\text{CO}_2$ ) in aqueous solutions. They can transport themselves through blood and deliver the loaded thrombin into the vasculature of wounds. They can halt severe hemorrhage in multiple animal models of intraoperative and traumatic bleeding. Following this strategy, self-propelling Janus particles are devised to improve the movement pattern by directing the driving force along a specific direction.<sup>53</sup> By releasing bubbles uniaxially, the Janus delivery system can reach the deep bleeding sites of liver and femoral artery hemorrhage models, promoting hemostasis in perforating and irregular wounds. Besides bubble

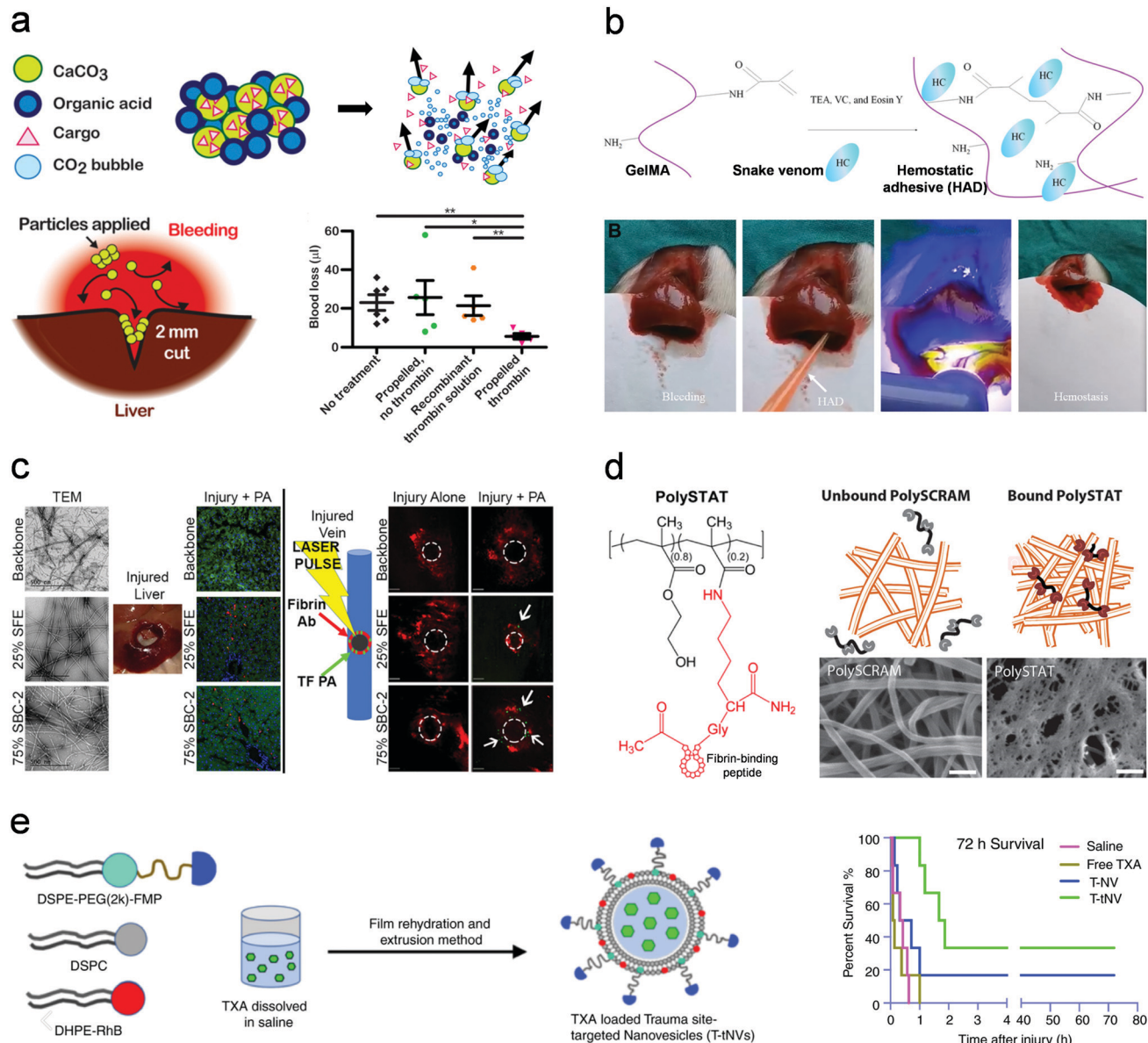


**Fig. 4** Hemostatic biomaterials based on coagulation factors, antifibrinolytics, and their synthetic analogs. (a) Water-triggered and gas-generating particles can transport through blood and deliver cargo like thrombin to wound beds.<sup>52</sup> Reproduced under the terms of the CC BY-NC Creative Commons Attribution 4.0 NonCommercial License. Copyright 2015, The Authors, published by American Association for the Advancement of Science. (b) Procoagulant snake venom is loaded into the methacrylated gelatin (GelMA) matrix crosslinked with visible light.<sup>55</sup> Reproduced under the terms of the CC BY-NC Creative Commons Attribution 4.0 NonCommercial License. Copyright 2021, The Authors, published by American Association for the Advancement of Science. (c) Nanofibers consist of peptide amphiphiles, conjugated with tissue factor-targeting sequences derived from factor FVII, and target hemorrhage sites including injured liver and vein.<sup>63</sup> Reproduced with permission. Copyright 2020, American Chemical Society. (d) PolySTAT carries a specific fibrin-binding peptide to mimic the function of FXIII to crosslink fibrin.<sup>45</sup> Reproduced with permission. Copyright 2015, American Association for the Advancement of Science. (e) Nanovesicles loaded with antifibrinolytic agents can anchor to bleeding sites and improve survival after liver hemorrhage.<sup>72</sup> Reproduced with permission. Copyright 2019, International Society on Thrombosis and Haemostasis.

propulsion, magnetic particles have been exploited as a thrombin-loaded system.<sup>54</sup> This enables sustained driving capability under magnetic guidance, delivering thrombin into perforating wounds and achieving superior hemostatic performance.

Similar to thrombin, the venom of snake *Bothrops atrox*, known as reptilase, can rapidly convert fibrinogen to fibrin. Therefore, the procoagulant activity of snake venom was utilized to develop a hemostatic hydrogel (Fig. 4b).<sup>55</sup> The reptilase

was encapsulated in gelatin methacryloyl (GelMA) hydrogels crosslinked by visible light. The hydrogels induce the activation and aggregation of platelets and efficiently transform fibrinogen into fibrin to achieve rapid hemostasis and seal the tissue.

Hemostatic products based on thrombin and fibrin are commercially available and widely used in the clinic. Gelatine-thrombin matrix sealants are commonly used to facilitate fibrin formation, promoting coagulation and minimising blood loss.



For example, Floseal (Baxter) and Surgiflo (Ethicon Endo-Surgery) are composed of a flowable gelatin matrix (bovine or porcine gelatin particles) and a human-derived thrombin component.<sup>56</sup> The two components are typically mixed immediately before use and directly injected into the bleeding sites. For the fibrin-based sealants, one of the best-known is TISSEEL (Baxter), which contains a formulation of fibrinogen and thrombin and can form a clot upon mixing and spraying at the injury sites.<sup>57</sup>

### 3.3 Other coagulation factor-based hemostats

Other coagulation factors part of the coagulation cascades also play an indispensable role in hemostasis. Factor VIII (FVIII) and Factor IX (FIX) are involved in the intrinsic pathway of thrombin generation, and their shortage can result in Hemophilia A and Hemophilia B, respectively. A variety of recombinant activated FVIII (*e.g.*, Kogenate) and FIX (*e.g.*, BeneFix) proteins have been developed to treat the bleeding in hemophilia patients.<sup>58,59</sup> Since Factor VII (FVII) is involved in the extrinsic pathway of thrombin generation, the recombinant activated FVII is one of the most notable recombinant coagulation factor products. Its use has demonstrated significant hemostatic performance in trauma, postpartum hemorrhage, and cardiac surgeries.<sup>60–62</sup>

Tissue factor (TF, also known as Factor III) is present in the adventitia of blood vessels, as well as epidermal and mucosal lining cells. Its exposure to blood after injuries triggers the extrinsic coagulation pathway *via* the interaction with FVII. Therefore, the TF can be utilized as a selective target for the delivery of hemostatic agents to the wound sites. As an example shown in Fig. 4c, a series of TF-targeting sequences were identified from the structure of FVII and incorporated into peptide amphiphile molecules, which further assemble into nanofibers. The injectable, targeted supramolecular nanotherapeutics localize selectively to the hemorrhage sites, decreasing blood loss by 35–59% in a liver hemorrhage model.<sup>63</sup>

Activated Factor XIII (FXIIIa) is a transglutaminase, which catalyzes amide bond formation between the lysine and glutamic acid residues of self-assembled fibrin protofibrils, thereby creating intra- and inter-fiber covalent crosslinks to strengthen and stabilize fibrin clots.<sup>64</sup> Congenital FXIII deficiency leads to severe bleeding, impaired wound healing, and spontaneous abortions. Administering FXIII at wound sites improves the adhesive strength of blood clots and reduces rebleeding in a rat model with femoral artery injury.<sup>21</sup> The efficacy and safety of recombinant FXIII have been demonstrated in treating congenital FXIII-A subunit deficiency in a Phase 3 prophylaxis trial.<sup>65</sup>

By mimicking the function of FXIII, a hemostatic polymer (PolySTAT) containing a pendant fibrin-binding peptide was synthesized (Fig. 4d).<sup>45</sup> PolySTAT can crosslink the fibrin within clots, resulting in a fortified and hybrid polymer network with enhanced resistance to enzymatic degradation. A rat trauma model showed that the intravenous administration of PolySTAT improved survival by reducing blood loss and resuscitation fluid requirements. By taking advantage of the crosslinking effect of FXIII, a synergetic hemostatic hydrogel composed of a self-assembling short peptide, *O*-carboxymethyl chitosan and

tissue transglutaminase was developed.<sup>66</sup> In this system, the transglutaminase not only crosslinks the short peptide, but also creates amide bonds between the peptide and chitosan due to less sequence specificity of the transglutaminase for amines.<sup>67,68</sup>

### 3.4 Antifibrinolytic agent-based hemostats

Antifibrinolytic agents can inhibit fibrinolysis and increase fibrin stability, therefore being widely used in trauma management and surgeries.<sup>69,70</sup> Examples include epsilon-aminocaproic acid (EACA), tranexamic acid (TXA), and aprotinin. Among them, TXA is the most acknowledged antifibrinolytic drug due to its safety and efficacy, which functions by blocking the lysine binding sites on plasminogen.<sup>71</sup> The targeted delivery of TXA is beneficial for addressing trauma-associated hemorrhage.<sup>72</sup> Researchers decorated the surface of liposomes with a fibrinogen-mimetic peptide (FMP), and encapsulated TXA within the nanovesicles (Fig. 4e). These intravenously administered nanovesicles can selectively anchor to the activated platelets at the bleeding sites, and wield their antifibrinolytic effect. The TXA-loaded nanovesicles maintained systemic safety *in vivo*, significantly reducing blood loss and improving survival in the rat liver hemorrhage model. Other studies include TXA-loaded microspheres, microparticles, and nanofibers made of chitosan, alginate, starch and gelatin for hemorrhage control applications.<sup>73–76</sup> However, it should be noted that increased rates of deep vein thrombosis in patients who receive TXA have been reported.<sup>77</sup>

## 4. Mechanical hemostatic biomaterials

In addition to biochemical hemostats, mechanical hemostats are under active development and receive increasing attention. Their progress is in part fueled by recent advances in related research areas, including hydrogels, bioadhesives and biofabrication. The convergence of disciplines leads to interdisciplinary approaches, allowing one to exert and control mechanical mechanisms, including absorption, agglutination, and adhesion, at the bleeding sites. A summary of mechanical hemostatic biomaterials is shown in Table 3. The design principles and applications of the mechanical hemostats are reviewed below.

### 4.1 Absorbent hemostats

A variety of absorbent materials have been developed for hemorrhage control, while some have been translated into the clinic. They generally constitute a hydrophilic dehydrated matrix with interconnected pores or channels (Fig. 5a). Such structures are formed with cryogelation, lyophilization, gas foaming, and sacrificial template leaching. The combination of chemical and structural properties enables the capacity to absorb a large amount of water from the blood, leaving concentrated blood components at the bleeding site that promote hemostasis.<sup>78</sup> Absorption involves mainly liquid transport and matrix expansion, thus categorized as a mechanical strategy; note that it takes place along with some biochemical reactions, for instance, blood clotting.

Table 3 Summary of mechanical hemostatic biomaterials

Hemostatic biomaterials	Hemostatic mechanism	Hemostatic efficacy	Application scenarios	Advantages and disadvantages
Conductive cryogels based on carbon nanotube (CNT) and glycidyl methacrylate (GMA) functionalized quaternized chitosan (QCSG) <sup>79</sup>	Absorbent hemostats – cryogels	Blood loss decreased from 24.3 g to 0.2 g and hemostatic time decreased from 25.0 min to 3.7 min in a rabbit liver defect lethal hemorrhage model	Covering the site with slight pressure, or through injection	Antibacterial, conductive, shape memory/recovery, and high blood uptake capacity; CNT amount required to be optimized
Capillary-mimicking composite hemostatic sponge made by carboxymethyl chitosan and sodium carboxymethylcellulose <sup>81</sup>	Absorbent hemostats – sponge	Hemostatic time of 73 s and blood loss of 0.57 g compared with positive control (gelatin sponge, 167 s and 1 g) and negative control (gauze, 360 s, 2.8 g), shown in a rat artery injury model	Covering the bleeding site	High liquid absorption capacity; long duration of preparation (at least 65 hours), requiring a wide temperature range (from a liquid nitrogen bath to 110 °C)
Self-expanding porous material XSTAT (RevMedx, Wilsonville, OR), consisting of cellulose sponges coated with chitosan <sup>82</sup>	Absorbent hemostats – expanding sponge	In a wound model, time of application decreases from 67 s (gauze) to 8 s (XSTAT), and hemorrhage reduces from 113 mL to 93 mL	Deploy sponge into wound by applicator	Quick self-expanding; slow removal for XSTAT (146 s) <i>versus</i> gauze (6.8 s)
Self-expanding porous composites consisting of carboxymethyl cellulose (CMC) and acetalized polyvinyl alcohol (PVA) <sup>83</sup>	Absorbent porous composite	In a rat liver injury model, blood loss and hemostatic time decrease from 429.3mg to 92.7mg and 202.8s to 77.9s, respectively	Inject to wound sites	Fast liquid-triggered self-expanding ability, and good expansion force; limited water absorption capacity and rate due to increasing CMC; non-compressible hemorrhage is required to be tested
Gelatin-coated expanded polycaprolactone (PCL) nanofiber sponge <sup>84</sup>	Absorbent hemostats – injectable nanofiber sponge	In a swine femoral artery hemorrhage model, blood loss and hemostatic time decrease from 751.6 g to 366.3 g and 696.9 s to 88.0 s, respectively	Injection using a syringe	Fast shape re-expansion and absorption of blood; more subjects are needed
Microchannelled alkylated chitosan sponge <sup>88</sup>	Absorbent hemostats – sponge	In swine liver injury model, blood loss reduced from 1140 mL (no treatment) to ~300 mL	Injection using a syringe	Fast shape re-expansion and absorption of blood; more subjects are needed
Chitosan <sup>90</sup>	Agglutination-based hemostats	In a lethal pig liver perforation wound model, the hemostatic time dropped from at least 10 min (untreated) to 2 min, while the total blood loss decreased from 153.0 g to 17.6 g	Cylindrical sponge compressed and filled into the wound cavity while squeezing free water out	Strong hemostatic capacity, antibacterial activity and improved tissue regeneration; complex fabrication for a hierarchical porous structure
Hydrophobically modified (hm) chitosan <sup>91</sup>	Agglutination-based hemostats	In a dog infrarenal aorta excise model, 4 in control (graft soaked in saline solution) experienced exsanguination and died, while the 7 treated with chitosan have mean blood loss of 43.57 mL	Grafts soaked in chitosan solution, then sewn onto the excised area	Prevent blood loss from porous vascular grafts, and fibroplasia for tissue repair; hemostatic time to be determined
Hyperbranched polyglycerols (HPGs) functionalized with sulfobetaine and quaternary ammonium <sup>92</sup>	Agglutination-based hemostats	In a rat femoral vein injury model, the bleeding time reduced from 50 s (saline control) to 4.5 s (hm-chitosan)	Dispersed through a syringe, or as bandage (for larger hemorrhage)	Low-cost yet effective, applicable in trauma centers; measurement of blood loss <i>in vivo</i> test should be done
Hydrogels composed of dodecyl-modified chitosan and benzaldehyde-terminated polyethylene glycol <sup>93</sup>	Agglutination-based hemostats	≥40% substitution of quaternary amine induced agglutination without red blood cell lysis	Polymer solution mixed with blood samples	Synthetic polymers with controlled positive charges for agglutination; animal studies required to prove hemostatic efficacy
Chitosan modified with catechol (CHI-C) <sup>98</sup>	Agglutination-based hemostats	Bleeding quickly stopped in mouse jugular vein puncture, femoral vein puncture, and a hemorrhaging liver model	Injection as a physical barrier	Blood agglutination, antibacterial, good biocompatibility; more quantitative measurements on blood loss and hemostatic time are needed
		In an anticoagulant treated rabbit model of liver resection bleeding, blood loss decreased from 64 g (gauze) to 9 g (CHI-C sponge)	Sponge applied to the bleeding site for coagulopathy hemorrhage	Proved hemostasis for human patients even with coagulopathic conditions; manual pressure was applied in the rabbit model; the human clinical trial lacks total blood loss comparison
		In pig liver injury model with coagulopathy, hemostasis time dropped from 16.6 s to 3.2 s, while total blood loss decreased from 348.6 mL to 123.4 mL		
		In a clinical study in patients with hepatectomy, the hemostasis time dropped to 168 s compared with market products (surgicel = 288 s, TachoSil = 180 s)		

Table 3 (continued)

Hemostatic biomaterials	Hemostatic mechanism	Hemostatic efficacy	Application scenarios	Advantages and disadvantages
Hydrogels based on tetra-PEG-NHS ester and tetra-PEG amine <sup>104</sup>	Adhesive hemostats	In a rabbit liver model, the hemostasis time reduced from at least 5 min (gauze) to less than 30 s. For porcine spleen massive hemorrhage, hydrogel gelled on the wound quickly and stopped bleeding after 5 min.	Hydrogel sealant	Hemostatic efficacy even in anticoagulated conditions; more quantitative measurement on total blood loss is required
Tough adhesives, with the adhesive surface of the bridging polymer (chitosan), and the dissipative matrix of the hydrogel (alginate-polyacrylamide) <sup>105</sup>	Adhesive hemostats	In a rat liver laceration model, blood loss drastically decreased from ~3600 mg (no treatment) to ~200 mg using tough adhesives	Tissue adhesives as a sealant on top of the injury site	Strong adhesion for prolonged periods; hemostatic time comparison to be determined
Barnacle-glue-inspired paste with microparticles of polyacrylic acid grafted with NHS ester embedded in oil <sup>106</sup>	Adhesive hemostats	For a rat hepatic injury model, the time to hemostasis drastically dropped from ~371 s to ~6 s, and blood loss from ~1327 mg to 84 mg. For rat cardiac injury model, time to hemostasis drastically dropped from 300 s to ~7 s, and blood loss from ~7.7 g to 0.6 g.	Bioadhesive paste as a sealant injected onto the bleeding site	By repelling blood, bioadhesive microparticles form strong adhesion; long-term safety and efficacy analysis are necessary
Aldehyde functionalized dextran sponge <sup>108</sup>	Adhesive hemostats	In a rabbit non-compressible liver hemorrhage model, the hemostasis time and blood loss weight decreased from >420 s to 240 s and 1.12 g to 0.31 g, respectively; for a femoral artery injury model, the hemostasis time decreased to <120 s compared with standard gauze (>180 s), and total blood loss also dropped from 7.8 g to 0.1 g.	Sponge applied to the bleeding site	Proper blood absorption and strong tissue adhesion; limited controllability over aldehyde modification
Photo-reactive adhesive composed of <i>o</i> -nitrobenzene modified hyaluronic acid (HA-NB) and methacrylated gelatin (GelMA) <sup>112</sup>	Adhesive hemostats	In a rabbit liver resection model, the blood loss decreased from ~230 mg to ~90 mg. In a pig carotid artery incision model, no more bleeding after 30 s when hemostatic forceps were taken away.	Injection of precursor solution and UV exposure	High blood burst pressure (up to 290 mmHg); may not be easy to apply UV irradiation at any possible bleeding site
Hyperbranched polymer with a hydrophobic backbone and hydrophilic adhesive catechol side branch <sup>119</sup>	Adhesive hemostats	In a rat liver bleeding model, the hemostatic efficacy increases from 26% (gauze) to 93%; blood loss dropped from 112 mg (blank) to 7.2 mg. In a pig liver deep puncture model, injection of liquid sealed the wound and stopped bleeding in 4 s.	Impregnated cotton swab treatment of the bleeding site; or injectable liquid agent	Strong adhesion to various materials; more quantitative measurement and comparison of the total blood loss are needed
Hydrogel composed of catechol-conjugated HA, thiourea-conjugated HA, and 4-arm thiolated PEG <sup>123</sup>	Adhesive hemostats	In pig upper gastrointestinal (GI) hemorrhage, hemostasis achieved within 2 min, and no rebleeding was observed at 30 min at the normal blood pressure	Endoscopic application to GI	Gelation at acidic pH suitable for upper GI hemorrhage; long-term maintenance of the hydrogels needs to be evaluated



**Fig. 5** Schematic and examples of absorbent hemostats. (a) Schematic of absorbent hemostats with interconnected pores or channels, which can absorb blood and/or expand to exert physical pressure on the wound for hemostasis. (b) A multifunctional cryogel composed of CNTs and quaternized chitosan demonstrates robust mechanical strength, rapid shape recovery and superabsorbent properties. It promoted clotting for non-compressible hemorrhage and wound healing.<sup>79</sup> Reproduced under the terms of the CC BY Creative Commons Attribution 4.0 International License. Copyright 2018, The Authors, published by Springer Nature. (c) The PCL nanofiber hemostatic matrices were fabricated by electrospinning, gas foaming and functional coating. They are packed for use as expandable hemostats.<sup>84</sup> Reproduced with permission. Copyright 2018, Elsevier. (d) An alkylated chitosan sponge with hierarchical microchannels and micropores was fabricated by template leaching and freeze drying. It not only achieved efficient hemostasis, but also promoted cell infiltration, vascularization, and tissue integration.<sup>88</sup> Reproduced under the terms of the CC BY Creative Commons Attribution 4.0 International License. Copyright 2021, The Authors, published by Springer Nature.

These effects are manifested with a multifunctional cryogel (Fig. 5b), composed of carbon nanotubes (CNTs), methacrylated quaternized chitosan, and diacrylated Pluronic F127.<sup>79</sup> Formation of a hydrophilic polymer network around ice crystals leads to the interconnected and macroporous structure after thawing of ice crystals, which endows the cryogel with superabsorbent properties. The incorporation of CNTs as an additive not only enhances the mechanical performance of the porous cryogel, but also provides pro-coagulant function by interacting with platelets. These cryogels tested in rodent and rabbit bleeding models demonstrate rapid blood absorption, high blood uptake capacity and blood-triggered shape recovery, thereby achieving excellent hemostasis. Also, the specific formulation provides the conductive and antibacterial properties to promote wound healing, following the hemostasis. Another absorbent hemostat with a highly sophisticated porous structure was prepared with a technique called ice-segregation-induced self-assembly (ISISA).<sup>80</sup> Briefly, the precursor solution composed of carboxymethyl chitosan and sodium carboxymethylcellulose was unidirectionally immersed in liquid nitrogen.<sup>81</sup> Ice crystals grow along the temperature gradient, resulting in a capillary-mimicking sponge with aligned microchannels after freeze-drying. This unique structure enables liquid suction, thus achieving superior liquid absorption capacity and rapid hemostasis.

Self-expanding porous materials can uptake the liquid and apply swelling pressure at the bleeding site. This synergy of

absorption and tamponade effects is shown to afford efficient hemostasis. This mechanism is embodied with XSTAT (RevMedx), an FDA-approved product for military use.<sup>82</sup> This material, consisting of cellulose sponges coated with chitosan, can absorb blood and quickly expand several times volumetrically to achieve hemostasis. Similar materials are prepared by gas foaming. For example, a porous composite made of acetalized polyvinyl alcohol (PVA) and cellulose fibers was fabricated with supercritical CO<sub>2</sub> as a foaming agent and sequential freeze drying. The composite demonstrated excellent absorption capacity, fast self-expanding ability, and high hemostatic efficacy in a swine femoral artery hemorrhage model.<sup>83</sup> Another example is a polycaprolactone (PCL) nanofiber hemostatic matrix (Fig. 5c).<sup>84</sup> They were prepared by electrospinning, expanded by immersion in NaBH<sub>4</sub> solution, and then coated with gelatin and thrombin. The packed nanofiber sponge can be injected, absorb water or blood, and quickly expand to its original shape at wound sites. Other self-expanding materials include a quaternized hydroxyethyl cellulose/mesocellular silica foam hydrogel sponge,<sup>85</sup> and an expandable PVA/gelatin composite sponge.<sup>86</sup> A common issue associated with absorbent hemostats is worth noting, that is, limited biodegradability. For example, XSTAT is non-degradable which necessitates manual removal from the wound bed, which risks rebleeding and prolongs the procedural time.<sup>87</sup>

Beyond hemostasis, tissue regeneration is an important consideration for hemostat design. In this regard, the porous hemostats can facilitate and guide tissue regeneration with a designer microstructure. The feasibility was demonstrated with a degradable chitosan sponge with controlled microchannels, produced through leaching of embedded 3D-printed microfibers (Fig. 5d);<sup>88</sup> the chitosan was also modified with hydrophobic alkyl chains to enhance its hemostatic and anti-infection properties. The sponge possessed a hierarchical porous structure, featuring both microchannels ( $136.5 \pm 17.8 \mu\text{m}$ ) and micropores ( $8.3 \pm 0.8 \mu\text{m}$ ), which favored blood absorption, nutrient transport, and cell infiltration. Such materials demonstrated strong hemostatic capacity, antibacterial activity, and importantly promotion of liver parenchymal cell infiltration, vascularization, and tissue integration in a rat liver defect model. Another biodegradable hemostat is an expandable dry cryogel with photothermal antibacterial activity based on polydopamine crosslinked chitosan,<sup>89</sup> which was shown to halt hemorrhage arising from lethal deep-wounds and coagulopathy, and to facilitate tissue regeneration.

#### 4.2 Agglutination-based hemostats

Agglutination is a process in which blood components such as red blood cells are crosslinked by exogenous biomaterials

into solid gels (Fig. 6a). Given ample interactions amenable for crosslinking, agglutination hemostats have been explored with different mechanisms such as electrostatic attraction and hydrophobic association.<sup>90–93</sup> Agglutination relies on the intrinsic physical and chemical properties of blood components so that agglutination hemostats are applicable to blood coagulopathies.

Many agglutination hemostats are based on polycations, polymers carrying positive charges.<sup>90,94</sup> A notable example is chitosan, carrying positively charged amine groups at acidic and neutral pH, which can bind electrostatically with negatively charged membranes of RBCs and platelets;<sup>95,96</sup> other recognized effects of chitosan include activating platelets and influencing coagulation cascades.<sup>97</sup> The resulting aggregates of blood and polymers serve as mechanical plugs formed at the bleeding sites. But the mixing of heparinized blood and chitosan solution cannot form a self-supporting gel due to the weak electrostatic interaction (Fig. 6b).<sup>91,93</sup> A remedy for this issue is the incorporation of hydrophobic alkyl side chains, called the hydrophobe, onto the chitosan so that the hydrophobe could insert into the membranes of blood cells and connect the cells into a network (Fig. 6b).<sup>91</sup> The additional hydrophobic association was shown to strengthen the agglutination product, and the hydrophobically modified chitosan (hm-chitosan) was

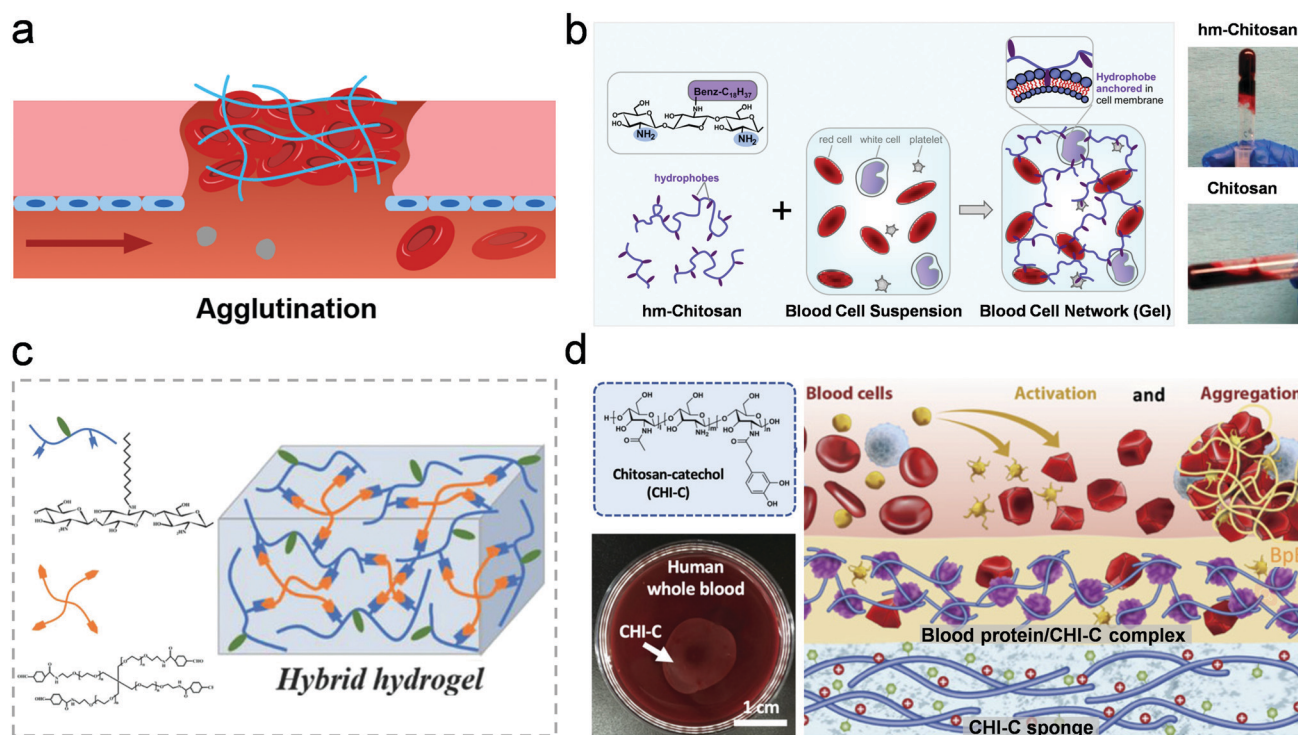


**Fig. 6** Design and examples of agglutination-based hemostats. (a) Agglutination involves crosslinking blood components such as blood cells and proteins with biomaterials into a solid gel. (b) Chitosan conjugated with hydrophobes (alkyl side chains) can fuse with blood cell membranes via hydrophobic association, thereby crosslinking blood cells into a solid gel. The hm-chitosan can turn the anticoagulated blood into a self-supporting gel, whereas chitosan cannot.<sup>91</sup> Reproduced with permission. Copyright 2010, Elsevier. (c) A hydrogel was made of dodecyl-modified chitosan and crosslinked by benzaldehyde-terminated polyethylene glycol. The hydrophobic tails on chitosan can aggregate blood cells for hemostasis.<sup>93</sup> Reproduced with permission. Copyright 2018, Wiley-VCH. (d) Chitosan modified with catechol (i.e., CHI-C) can complex with plasma proteins and cells, forming a barrier layer to seal bleeding sites.<sup>98</sup> Reproduced under the terms of the CC BY-NC Creative Commons Attribution 4.0 NonCommercial License. Copyright 2021, The Authors, published by American Association for the Advancement of Science.

found to rapidly solidify liquid blood and achieve hemostatic efficacy with rat and pig models. As shown in Fig. 6c, a hydrogel composed of dodecyl-modified chitosan and benzaldehyde-terminated polyethylene glycol demonstrated outstanding blood cell agglutination, hemostasis, tissue adhesion and cell recruitment functions owing to the hydrophobic tails on chitosan.<sup>93</sup> A similar approach was also utilized in the micro-channel structured sponge as discussed in Section 4.1, and the incorporation of alkyl chains increased the hemostatic and anti-infective abilities of chitosan.<sup>88</sup>

Besides the hydrophobe, catechol is grafted onto the backbone of chitosan. The catechol is a versatile moiety inspired by mussel adhesion, which will be discussed in detail in Section 4.3. The incorporation of catechol can enhance the interaction between chitosan and blood components (*e.g.*, proteins and cells). Fig. 6d shows a coagulopathy-independent hemostat, where the chitosan is modified with catechol and freeze-dried into a sponge;<sup>98</sup> provided some plasma proteins, the synergy of catechol and positive charges instantly triggers the formation of adhesive membranes for hemostasis. The dissolved catechol-chitosan forms a complex with plasma proteins and blood cells *via* ionic/covalent/hydrogen bonds and hydrophobic interactions. The hemostatic efficacy was demonstrated in animal bleeding models, independent of blood conditions, and the first-in-human hepatectomy.

In addition to chitosan, researchers have developed synthetic polymers with controlled positive charges for agglutination. For example, a library of hyperbranched polyglycerols (HPGs) were synthesized and further functionalized with zwitterionic sulfobetaine and cationic quaternary ammonium ligands.<sup>92</sup> These polymers with  $\geq 40\%$  substitution of quaternary amines induced agglutination without red blood cell lysis, therefore promoting hemostasis independent of normal blood clotting.

### 4.3 Adhesive hemostats

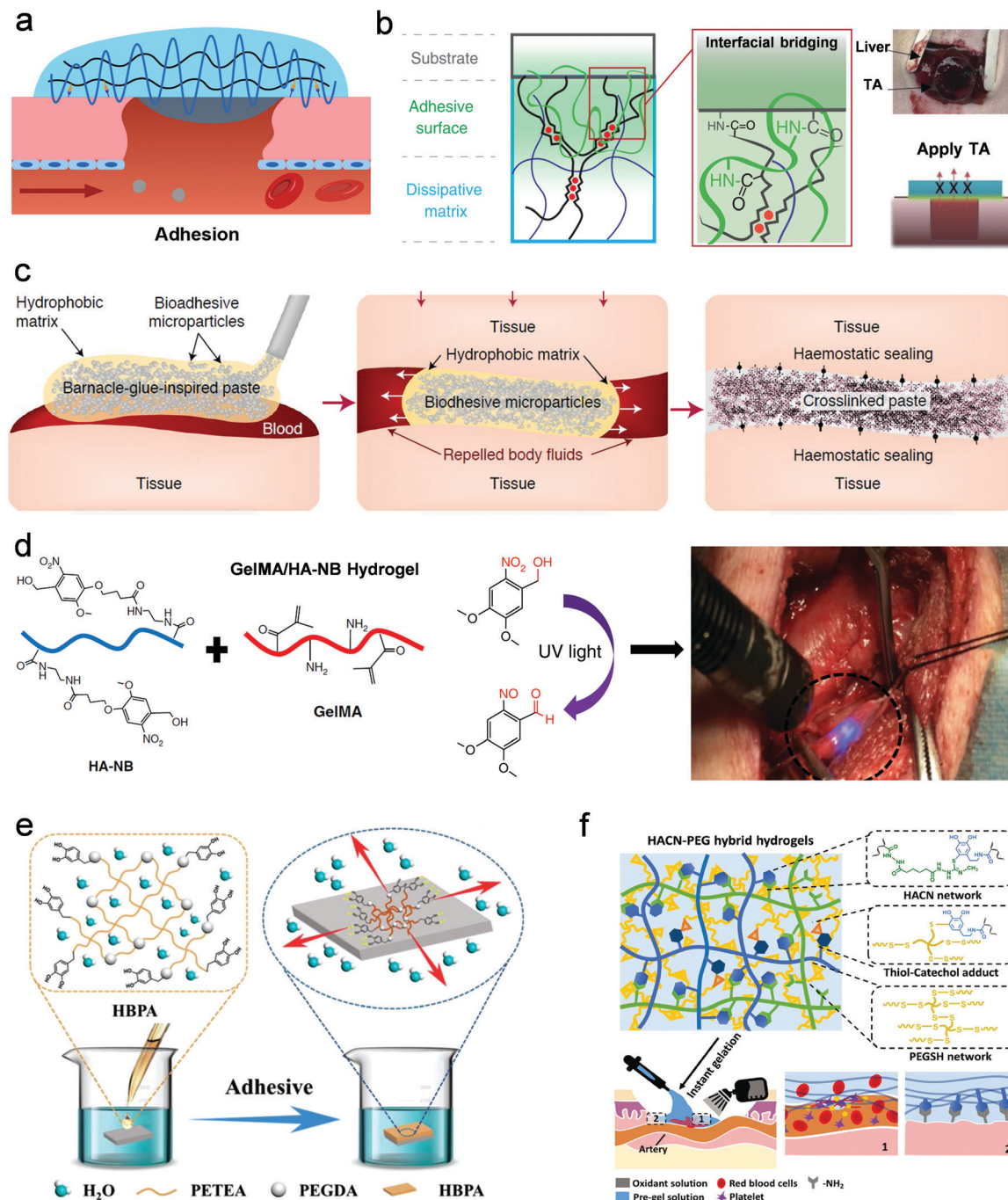
Bioadhesives have been increasingly used for hemostatic management in recent years.<sup>7,99–101</sup> They can adhere to tissues *via* covalent bonding with tissue surface groups (*e.g.*, amine, carboxyl and thiol) and/or *via* non-covalent interactions (*e.g.*, ionic bonds and hydrogen bonds), thereby sealing the wound and providing a mechanical barrier to stop bleeding (Fig. 7a). A summary of chemistry commonly used in adhesive hemostats is listed in Table 4. A group of such materials based on *N*-hydroxysuccinimide ester (NHS ester) can react with primary amines and thiols.<sup>102–104</sup> A notable example is a commercially available tissue sealant, Coseal (Baxter), composed of tetra-PEG-NHS ester and tetra-PEG-thiol. This product has a limited shelf life as the thiol group is prone to oxidation. The remedy is tetra-PEG-amine, which crosslinks with tetra-PEG-NHS ester to form a hemostatic sealant.<sup>104</sup> Further optimization of the molecular structure of tetra-PEG-NHS ester leads to fast degradation and better biocompatibility. The resulting sealant demonstrates strong tissue adhesion and outstanding hemostatic capabilities even under anticoagulated conditions.

The performance of many commercial sealants is found to be limited by their brittle matrix and weak adhesiveness.

These limitations are overcome with recent progress, including tough adhesives (TA) developed by us for wound closure and hemostasis.<sup>105</sup> As shown in Fig. 7b, the TA consists of two layers: an adhesive surface and a dissipative matrix. The adhesive surface containing a positively charged polymer (*e.g.*, chitosan) binds with biological tissues through electrostatic interaction, covalent bonds, and physical interpenetration. The matrix made of a double-network hydrogel further enhances the adhesion by amplifying energy dissipation during debonding. Their synergy leads to strong adhesion on blood-exposed tissues with an adhesion energy of up to  $1116 \text{ J m}^{-2}$ . When applied to a heavily bleeding liver, TA significantly reduces blood loss and sealed the wound.

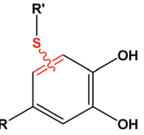
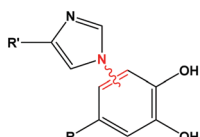
Blood and other body fluids often impair the adhesion performance of bioadhesives. This issue can be addressed by either absorbing the liquid into the adhesive matrix as discussed in Section 4.1 or repelling the fluid from the wound site. As an example shown in Fig. 7c, a hemostatic paste inspired by barnacle glue consists of a blood-repelling hydrophobic oil matrix, containing bioadhesive microparticles made of polyacrylic acid grafted with NHS ester (PAAc-NHS ester).<sup>106</sup> Under gentle compression, the hydrophobic matrix repels the blood, enabling the compacted microparticles to bind with one another and with the tissue surface. With rapid crosslinking, it can seal blood-covered tissues in less than 15 seconds, achieving high burst pressure (350 mmHg), adhesion strength (30–70 kPa), and adhesion energy ( $150\text{--}300 \text{ J m}^{-2}$ ). The hemostatic paste was shown to outperform commercial hemostatic agents in treating bleeding porcine aortas *ex vivo* and bleeding heart and liver tissues in rats and pigs *in vivo*.

The second class of adhesive hemostats is reliant on aldehyde groups and the Schiff base reaction (Table 4). A commonly used approach is to introduce aldehyde groups into polysaccharides (*e.g.*, alginate, dextran, chitosan, and cellulose) *via* sodium periodate oxidation.<sup>107–109</sup> For example, an aldehyde dextran sponge enabled proper blood absorption ( $47.7 \text{ g g}^{-1}$ ) and strong tissue adhesion ( $\sim 100 \text{ kPa}$ );<sup>108</sup> its efficacy in hemostasis and blood loss reduction was demonstrated in the ear vein, femoral artery and liver injuries of rabbit models. Another example is a bioadhesive hydrogel composed of an aldehyde-cellulose nanocrystal and catechol-chitosan.<sup>110</sup> It can be injected into the internal and irregular bleeding sites and bone defective areas, and then rapidly self-heal (within 2 min) to a hydrogel due to the dynamic Schiff-base linkages. Strong bioadhesion was also formed by exploiting the bioadhesive properties of catechol and aldehyde. However, the periodate oxidation of polysaccharides has limitations, including side reactions, overoxidation and free radical depolymerization, which leads to poor controllability over the aldehyde modification.<sup>111</sup> To this end, a photo-reactive adhesive composed of *o*-nitrobenzene modified hyaluronic acid (HA-NB) and methacrylated gelatin was developed (Fig. 7d).<sup>112</sup> The modified HA generated an *o*-nitrosobenzaldehyde group under UV irradiation and rapidly bonded with amines on the tissue surface. The resulting sealing can withstand up to 290 mmHg blood pressure and stop pressurized blood flows from pig carotid arteries and hearts.



**Fig. 7** Design and examples of adhesive hemostats. (a) Bioadhesives adhere to tissues via covalent bonding and/or non-covalent interactions, therefore sealing the wound mechanically to prevent blood loss. (b) Tough adhesives (TA) are constructed with an adhesive surface and a dissipative matrix and are capable of forming strong and robust adhesion with tissues. When applied to an injured liver, TA can reduce blood loss and seal the wound.<sup>105</sup> Reproduced with permission. Copyright 2017, The Authors, published by American Association for the Advancement of Science. (c) A barnacle-glue-inspired paste contains bioadhesive microparticles dispersed in a hydrophobic oil. When applied to the bleeding sites under gentle compression, the paste can repel blood or body fluid to form robust adhesion.<sup>106</sup> Reproduced with permission. Copyright 2021, The Authors, published by Springer Nature. (d) A photo-reactive adhesive composed of *o*-nitrobenzene modified hyaluronic acid (HA-NB) and methacrylated gelatin (GelMA) can solidify and generate aldehyde groups for bioadhesion under UV irradiation.<sup>112</sup> Reproduced under the terms of the CC BY Creative Commons Attribution 4.0 International License. Copyright 2019, The Authors, published by Springer Nature. (e) A hyperbranched polymer with a hydrophobic backbone and hydrophilic catechol side branches can quickly form coacervates upon contact with water and drain off the surface fluid, thus exposing catechol for bioadhesion.<sup>119</sup> Reproduced with permission. Copyright 2019, Wiley-VCH. (f) Modified HA and PEG form an interpenetrating network independent of environmental pH for gastrointestinal hemorrhage control.<sup>123</sup> Reproduced with permission. Copyright 2021, Wiley-VCH.

Table 4 A summary of chemistry used in adhesive hemostats

Adhesive functional groups	Tissue functional groups	Chemical reactions	Advantages and disadvantages	Ref.	
NHS-ester 	Amine $R'-NH_2$	Amide 	Thioester 	High reactivity and formation of a strong covalent bond Susceptibility to hydrolysis	102–106
Aldehyde 	Thiol $R'-SH$	Imine 	Hemithioacetal 	Dynamic covalent bond favorable for self-healing Poor controllability over aldehyde modification	107–110 112
Catechol 	Amine $R'-NH_2$	Schiff base reaction or Michael addition 		Versatile chemistry with a variety of tissue functional groups	113–117 119 and 120 123
	Thiol $R'-SH$	Michael addition 		Oxidation process required to generate the reactive quinones	
	Imidazole 				

Another extensively used functional group as shown in Table 4 is catechol or polyphenol, which can bind with nucleophiles (e.g., amines, thiols and imidazoles) present on tissues to achieve bioadhesion.<sup>113–118</sup> Fig. 7e illustrates a hyperbranched polymer with a hydrophobic backbone and hydrophilic adhesive catechol side branch.<sup>119</sup> Upon contacting water, the hydrophobic chains self-aggregate quickly into coacervates, displacing water molecules at the interface, thus exposing and attaching catechol groups to tissues. Meanwhile, the hydrophobic alkylamine chains contribute to blood clotting through the agglutination effect. These effects allow the injectable sealant to rapidly stop visceral bleeding, especially hemorrhage from a deep wound.

The mechanical performance of hemostats can be improved with a double-network design for the adhesive matrix. The efficacy can be seen with the TA discussed above. Also, a hemostatic sealant was made with catechol-modified methacrylated chitosan and methacrylated chitosan, exhibiting high mechanical performance *via* the simultaneous catechol-Fe<sup>3+</sup> chelation and light-induced crosslinking of carbon-carbon double bonds.<sup>120</sup> The catechol-Fe<sup>3+</sup> complex can substantially enhance the adhesion of the hydrogel to biological tissues. Despite hemostasis being validated in a hemorrhaging liver model, the gelation based on catechol-Fe<sup>3+</sup> coordination is pH-dependent: the binding stoichiometry changes from 1:1 at low pH ( $\leq 5$ , no crosslinking) to 3:1 at increased pH ( $\geq 7$ , stable gels).<sup>121</sup> This dependence complicates its application in acidic tissue environments, such as gastric tissues. As a remedy, a thiourea-catechol reaction was exploited to

desensitize the pH.<sup>122</sup> Specifically, the formulations include catechol-conjugated HA, thiourea-conjugated HA, and 4-arm thiolated PEG, where two intertwined networks of HA and PEG are formed by catechol-thiourea coupling and disulfide bonds, respectively (Fig. 7f).<sup>123</sup> Such adhesive hydrogels achieve endoscopic hemostasis against upper gastrointestinal (GI) hemorrhage in pigs and remain adherent at the bleeding wound for 48 hours, indicating sustained hemostatic function *in vivo*.

## 5. Discussion and outlook

Critical clinical needs for treating noncompressible hemorrhage drive the rapid development of hemostatic biomaterials. Mounting evidence supports their potential to supplement and even substitute the standard of care and blood transfusion, under the conditions of hemorrhage and coagulopathies where normal coagulation is impaired. Intensive research efforts so far have reported the general principles to rationally design hemostatic biomaterials, as well as important considerations for clinical translation. But a few barriers remain toward the ultimate translation of these materials into the clinic. Below we first discuss the design considerations and then the challenges and immediate opportunities in the field.

### 5.1 Rational design and translational considerations

The clinical requirements for managing noncompressible hemorrhage steer the design and applications of hemostatic



biomaterials. This severe condition often occurs in pulmonary, solid abdominal organ, major vascular, or pelvic trauma.<sup>124</sup> The current treatment involves operative intervention, while the probability of death increases by approximately 1% for each 3 min delay to surgery.<sup>125</sup> Hemostatic biomaterials are thus under critical demand for pre-hospital hemorrhage control at point-of-injury or during transport, where the hemostatic agents are expected to be storable, easily administrated even by a layperson under austere conditions, and effectively control bleeding before further definitive management.<sup>126</sup> Intraoperatively, the hemostatic biomaterials are used as an adjunct or alternative to standard surgical techniques, including electrocautery, vessel ligation, and suturing. Injectable and biodegradable hemostats are preferable and particularly useful for diffuse nonanatomic bleeding (*e.g.*, cut surface of solid organs) and sensitive bleeding sites (*e.g.*, nerves). Importantly, coagulopathy that frequently occurs after trauma and due to congenital or disease-associated conditions underscores the importance of coagulation-independent hemostats. Postoperatively, the biological functions of hemostatic biomaterials such as anti-infection and pro-healing are beneficial for wound healing. These considerations should be taken into account for the rational design of hemostatic biomaterials, potentiating a full spectrum hemorrhage management from prehospital control to postoperative care.

Besides hemostatic efficacy, important translational considerations of hemostatic biomaterials include safety, regulatory approval, as well as cost and scale-up production. The main safety issues associated with current hemostatic biomaterials include the transmission and infection of blood-borne pathogens, thromboembolic complications and immunological responses.<sup>126</sup> While the infection risk could be mitigated by rigorous screening tests and manufacture processes, deep-vein thrombosis was reported followed by administration of TXA and antibody-triggered severe coagulopathy has been linked with the use of bovine thrombin. Tissue damage and inhibition of healing are also concerns of some local hemostatic agents. Translational formulations of hemostats should consult with the regulatory use of the biomaterials, especially those approved by the Food and Drug Administration (FDA) for hemostatic applications. The existing hemostats approved by the FDA are mainly based on blood components (*e.g.*, platelets, fibrin, and thrombin), proteins (*e.g.*, collagen, gelatin, and albumin) and polysaccharides (*e.g.*, chitosan, cellulose, and starch). In the case of “substantially equivalent” predicate devices, the FDA 510(k) process could be pursued for lower regulatory requirements. For many hemostatic materials that are implanted in the body and reside for a long period of time, they are generally classified as high-risk medical devices (for example, as Class III by the FDA) and undergo some of the most stringent regulatory controls for human approval.<sup>127</sup> The risk, high costs and long timeline associated with clinical trials and regulatory approval are barriers for the translation of hemostatic biomaterials. Beyond the FDA approval, attention should be paid to the sales-force strategy and post-market studies to ensure successful translation and commercialization.

## 5.2 Remaining challenges

First, there are knowledge gaps on the mechanics of blood clots. In particular, fracture mechanics of blood clots is a burgeoning area of research; recent interest surged in part due to the advances in fracture mechanics of soft materials such as hydrogels and bioadhesives.<sup>25,128</sup> Another impetus is the increased risk of people infected with COVID-19 for developing thrombosis or blood clots in the veins. Many open questions remain, for instance, on how the blood components influence clot fracture. The adhesion fracture of blood clots on biological tissues and hemostatic biomaterials is unexplored, as well as the response of blood clots against cyclic loading. These answers to address the foregoing questions could help advance the design and performance of hemostatic biomaterials.

Another critical gap to fill is between *in vitro* testing (under idealized test conditions) and *in vivo* performance (involving animals). There are critical needs to standardize the testing conditions. Recognized are differences between the *in vitro* and *in vivo* formed blood clots, for instance, in terms of microstructure and composition. The boundary conditions of mechanical tests differ from *in vivo* conditions. Predicting the hemostatic performance from the fundamentals is challenging. Further research is needed to link, if possible, the mechanical properties (*e.g.*, stiffness, toughness and adhesion energy) with the hemostatic outcome. The endeavour is likely to resort to a finite element simulation and testing platform capable of recapitulating physiological conditions such as blood flow and pressure.

Another challenge is establishing appropriate animal bleeding models, as well as the medical standards of hemostatic experiments and outcomes. As can be seen in this review, the widely used animal models are based on mice, rats and rabbits. The assessment metrics include the bleeding time, blood loss and survival rate. However, the small animal models are inadequate to recapitulate the features of noncompressible hemorrhage due to their physiological and anatomical dissimilarities to humans, thus providing limited evidence for hemostatic performance.<sup>7</sup> Also, it is worth noting that comparing various biomaterials and technologies in different studies is challenging due to the large heterogeneity in the animal models used and outcomes evaluated. Therefore, standardized animal models and measurement criteria need to be established. Large animal models such as swine models are preferable, where more criteria such as the mean arterial pressure (MAP), heart rate, end tidal CO<sub>2</sub> (EtCO<sub>2</sub>), blood coagulation panel parameters, and serum lactate concentrations can be used to determine the grade of hemorrhage and evaluate the hemostatic efficacy of biomaterials.<sup>129</sup>

## 5.3 Immediate opportunities

The next-generation biomimetic platelets are expected to exert more bioactive functions to promote healing, and meanwhile lower the cost for practical translation. The existing artificial platelets have recapitulated some features of native counterparts, but active contraction and triggered granule release are

still beyond reach. Realizing these functions could benefit from advances in other areas, including stimuli-responsive polymers, controlled drug delivery and biomolecular motors.<sup>130–132</sup>

Besides platelets, other blood components provide other routes to strengthen clots and better hemostatic outcomes. Among them, RBCs are appealing due to their large volume ratio in blood (~45%) and underappreciated role in hemostasis. The mechanical contribution of RBCs to the clot fracture was reported recently, which could be further enhanced by cross-linking strategies to mechanically integrate RBC within clots. As such, transforming these commonly considered bystanders into active contributors for hemostasis might lead to a new class of hemostatic technologies.

There are opportunities to mechanically engineer the blood clots formed by or interfaced with hemostatic biomaterials. It is critical as the existing strategies such as electrostatic interaction and hydrophobic interaction, as discussed above, lead to mechanically weak clots and hemolysis. The catechol-based approach complexes unselectively with plasma proteins and therefore consumes the essential coagulant proteins such as fibrinogen, impairing the formation of a fibrin network and the final mechanical properties of blood clots. Engineering selective and strong bonds within the clot is a promising alternative to explore. Improving the mechanical properties of blood clots could enable better hemostasis and lower rebleeding risks.

Beyond hemostasis, downstream biological processes post injury, such as wound healing, tissue regeneration, and infection mitigation, should be accounted for when developing hemostatic biomaterials. Whereas the existing hemostats are preliminarily designed to halt bleeding, the future materials could promote healing and regeneration. To facilitate this aim, it is important to study how hemostatic biomaterials and their degradation products interact with cells, bacteria, and host tissues; in particular, the immune response and potential immunomodulation effects exerted by hemostats require further investigation. As hemostats play a multifaceted role in trauma and wound care, transdisciplinary efforts are expected to invent and translate the life-saving technologies of hemostatic biomaterials.

## Conflicts of interest

There are no conflicts to declare.

## Acknowledgements

This work was supported by the New Frontiers in Research Fund - Exploration (grant NFRFE-2018-00751), Canadian Institutes of Health Research Project grant (CIHR PJT-180232), and the Natural Sciences and Engineering Research Council of Canada (grant RGPIN-2018-04146). J. L. acknowledges the support from Canada Research Chairs program. Shiyu Liu and Sum Lau acknowledge the support from McGill Doctoral Scholarship and Mitacs Globalink Research Internship, respectively.

## References

- D. A. Hickman, C. L. Pawlowski, U. D. S. Sekhon, J. Marks and A. S. Gupta, *Adv. Mater.*, 2018, **30**, 1700859.
- E. Y. Koh, B. T. Oyeniya, E. E. Fox, M. Scerbo, J. S. Tomasek, C. E. Wade and J. B. Holcomb, *Am. J. Surg.*, 2019, **218**, 501–506.
- B. J. Eastridge, R. L. Mabry, P. Seguin, J. Cantrell, T. Tops, P. Uribe, O. Mallett, T. Zubko, L. Oetjen-Gerdes, T. E. Rasmussen, F. K. Butler, R. S. Kotwal, J. B. Holcomb, C. Wade, H. Champion, M. Lawnick, L. Moores and L. H. Blackbourne, *J. Trauma Acute Care Surg.*, 2012, **73**, S431–S437.
- C. C. Clifford, *Mil. Med.*, 2004, **169**, 8–10.
- X. X. Wang, Q. Liu, J. X. Sui, S. Ramakrishna, M. Yu, Y. Zhou, X. Y. Jiang and Y. Z. Long, *Adv. Healthcare Mater.*, 2019, **8**, 1900823.
- Y. Chen, L. Wu, P. Li, X. Hao, X. Yang, G. Xi, W. Liu, Y. Feng, H. He and C. Shi, *Macromol. Biosci.*, 2020, **20**, 1900370.
- S. Pourshahrestani, E. Zeimaran, N. A. Kadri, N. Mutlu and A. R. Boccaccini, *Adv. Healthcare Mater.*, 2020, **9**, 2000905.
- C. Zheng, Q. Zeng, S. Pimpi, W. Wu, K. Han, K. Dong and T. Lu, *J. Mater. Chem. B*, 2020, **8**, 5395–5410.
- L. Wang, X. You, C. Dai, T. Tong and J. Wu, *Biomater. Sci.*, 2020, **8**, 4396–4412.
- D. Li, J. Chen, X. Wang, M. Zhang, C. Li and J. Zhou, *Front. Bioeng. Biotechnol.*, 2020, **8**, 926.
- B. Guo, R. Dong, Y. Liang and M. Li, *Nat. Rev. Chem.*, 2021, **5**, 773–791.
- M. Wu, K. K. and M. Thiagarajan, *Annu. Rev. Med.*, 1996, **47**, 315–331.
- Z. M. Ruggeri and G. L. Mendolicchio, *Circ. Res.*, 2007, **100**, 1673–1685.
- K. Tomokiyo, Y. Kamikubo, T. Hanada, T. Araki, Y. Nakatomi, Y. Ogata, S. M. Jung, T. Nakagaki and M. Moroi, *Blood*, 2005, **105**, 1078–1084.
- K. Broos, H. B. Feys, S. F. De Meyer, K. Vanhoorelbeke and H. Deckmyn, *Blood Rev.*, 2011, **25**, 155–167.
- M. Hoffman, *J. Thromb. Thrombolysis*, 2003, **16**, 17–20.
- H. H. Versteeg, J. W. Heemskerk, M. Levi and P. H. Reitsma, *Physiol. Rev.*, 2013, **93**, 327–358.
- P. A. Evans, K. Hawkins, P. R. Williams and R. L. Williams, *J. Non-Newton. Fluid Mech.*, 2008, **148**, 122–126.
- V. Kumar and J. R. Chapman, *J. Extra-Corpor. Technol.*, 2007, **39**, 18–23.
- R. Tran, D. R. Myers, J. Ciciliano, E. L. Trybus Hardy, Y. Sakurai, B. Ahn, Y. Qiu, R. G. Mannino, M. E. Fay and W. A. Lam, *J. Cell. Mol. Med.*, 2013, **17**, 579–596.
- K. Y. T. Chan, A. S. M. Yong, X. Wang, K. M. Ringgold, A. E. John, J. R. Baylis, N. J. White and C. J. Kastrup, *Sci. Rep.*, 2020, **10**, 20116.
- G. P. Sugerma, S. H. Parekh and M. K. Rausch, *Soft Matter*, 2020, **16**, 9908–9916.
- G. P. Sugerma, S. Kakaletsis, P. Thakkar, A. Chokshi, S. H. Parekh and M. K. Rausch, *J. Mech. Behav. Biomed. Mater.*, 2021, **115**, 104216.

- 24 S. A. Mousa, S. Khurana and M. S. Forsythe, *Arterioscler., Thromb., Vasc. Biol.*, 2000, **20**, 1162–1167.
- 25 S. Liu, G. Bao, Z. Ma, C. J. Kastrup and J. Li, *Extreme Mech. Lett.*, 2021, **48**, 101444.
- 26 F. Ghezelbash, S. Liu, A. Shirazi-Adl and J. Li, *J. Mech. Behav. Biomed. Mater.*, 2022, **128**, 105101.
- 27 Y. Qiu, D. R. Myers and W. A. Lam, *Nat. Rev. Mater.*, 2019, **4**, 294–311.
- 28 R. Bai, J. Yang and Z. Suo, *Eur. J. Mech. A/Solids*, 2019, **74**, 337–370.
- 29 J. C. Chapin and K. A. Hajjar, *Blood Rev.*, 2015, **29**, 17–24.
- 30 P. Martínez-Botía, A. Acebes-Huerta, J. Seghatchian and L. Gutiérrez, *Transfus. Apher. Sci.*, 2020, **59**, 102864.
- 31 D. F. Stroncek and P. Rebullá, *The Lancet*, 2007, **370**, 427–438.
- 32 M. P. Lambert, S. K. Sullivan, R. Fuentes, D. L. French and M. Poncz, *Blood*, 2013, **121**, 3319–3324.
- 33 T. Nishiya, M. Kainoh, M. Murata, M. Handa and Y. Ikeda, *Blood*, 2002, **100**, 136–142.
- 34 G. Agam and A. A. Livne, *Eur. J. Clin. Invest.*, 1992, **22**, 105–112.
- 35 M. Levi, P. W. Friederich, S. Middleton, P. G. de Groot, Y. P. Wu, R. Harris, B. J. Biemond, H. F. Heijnen, J. Levin and J. W. ten Cate, *Nat. Med.*, 1999, **5**, 107–111.
- 36 B. S. Collier, K. T. Springer, J. H. Beer, N. Mohandas, L. E. Scudder, K. J. Norton and S. M. West, *J. Clin. Investig.*, 1992, **89**, 546–555.
- 37 J. P. Bertram, C. A. Williams, R. Robinson, S. S. Segal, N. T. Flynn and E. B. Lavik, *Sci. Transl. Med.*, 2009, **1**, 11ra22.
- 38 J. D. Humphries, A. Byron and M. J. Humphries, *J. Cell Sci.*, 2006, **119**, 3901–3903.
- 39 Y. Okamura, I. Maekawa, Y. Teramura, H. Maruyama, M. Handa, Y. Ikeda and S. Takeoka, *Bioconjugate Chem.*, 2005, **16**, 1589–1596.
- 40 Y. Okamura, T. Fujie, M. Nogawa, H. Maruyama, M. Handa, Y. Ikeda and S. Takeoka, *Transfus. Med.*, 2008, **18**, 158–166.
- 41 D. A. Hickman, C. L. Pawlowski, A. Shevitz, N. F. Luc, A. Kim, A. Girish, J. Marks, S. Ganjoo, S. Huang and E. Niedoba, *Sci. Rep.*, 2018, **8**, 1–14.
- 42 D. B. Cines, T. Lebedeva, C. Nagaswami, V. Hayes, W. Masefski, R. I. Litvinov, L. Rauova, T. J. Lowery and J. W. Weisel, *Blood*, 2014, **123**, 1596–1603.
- 43 A. C. Brown, S. E. Stabenfeldt, B. Ahn, R. T. Hannan, K. S. Dhada, E. S. Herman, V. Stefanelli, N. Guzzetta, A. Alexeev, W. A. Lam, L. A. Lyon and T. H. Barker, *Nat. Mater.*, 2014, **13**, 1108–1114.
- 44 Y. Gao, A. Sarode, N. Kokoroskos, A. Ukidve, Z. Zhao, S. Guo, R. Flaumenhaft, A. S. Gupta, N. Saillant and S. Mitragotri, *Sci. Adv.*, 2020, **6**, eaba0588.
- 45 L. W. Chan, X. Wang, H. Wei, L. D. Pozzo, N. J. White and S. H. Pun, *Sci. Transl. Med.*, 2015, **7**, 277ra29.
- 46 O. Kononova, R. I. Litvinov, A. Zhmurov, A. Alekseenko, C. H. Cheng, S. Agarwal, K. A. Marx, J. W. Weisel and V. Barsegov, *J. Biol. Chem.*, 2013, **288**, 22681–22692.
- 47 J. W. Weisel and R. I. Litvinov, *Blood*, 2013, **121**, 1712–1719.
- 48 J. W. Weisel and R. I. Litvinov, *Fibrous proteins: structures and mechanisms*, 2017, vol. 82, pp. 405–456.
- 49 C. Aubron, M. C. Reade, J. F. Fraser and D. J. Cooper, *J. Crit. Care*, 2014, **29**, 471.
- 50 O. Grottke and J. H. Levy, *Anesthesiology*, 2015, **122**, 923–931.
- 51 M. Franchini and G. Lippi, *Blood Transfus.*, 2012, **10**, 23.
- 52 J. R. Baylis, J. H. Yeon, M. H. Thomson, A. Kazerooni, X. Wang, A. E. John, E. B. Lim, D. Chien, A. Lee, J. Q. Zhang, J. M. Piret, L. S. Machan, T. F. Burke, N. J. White and C. J. Kastrup, *Sci. Adv.*, 2015, **1**, e1500379.
- 53 Q. Li, E. Hu, K. Yu, R. Xie, F. Lu, B. Lu, R. Bao, T. Zhao, F. Dai and G. Lan, *Adv. Funct. Mater.*, 2020, **30**, 2004153.
- 54 Q. Li, E. Hu, K. Yu, M. Lu, R. Xie, F. Lu, B. Lu, R. Bao and G. Lan, *Bioact. Mater.*, 2021, **6**, 4625–4639.
- 55 Y. Guo, Y. Wang, X. Zhao, X. Li, Q. Wang, W. Zhong, K. Mequanint, R. Zhan, M. Xing and G. Luo, *Sci. Adv.*, 2021, **7**, eabf9635.
- 56 M. Echave, I. Oyagüez and M. A. Casado, *BMC Surg.*, 2014, **14**, 111.
- 57 K. S. Vyas and S. P. Saha, *Expert Opin. Biol. Ther.*, 2013, **13**, 1663–1672.
- 58 A. Yoshioka, K. Fukutake, J. Takamatsu and A. Shirahata, *Int. J. Hematol.*, 2003, **78**, 467–474.
- 59 T. Lambert, M. Recht, L. Valentino, J. S. Powell, C. Udata, S. Sullivan and D. Roth, *Haemophilia*, 2007, **13**, 233–243.
- 60 U. Martinowitz, G. Kenet, E. Segal, J. Luboshitz, A. Lubetsky, J. Ingerslev and M. Lynn, *Transfus. Altern. Transfus. Med.*, 2001, **3**, 30–36.
- 61 M. Franchini, M. Franchi, V. Bergamini, M. Montagnana, G. L. Salvagno, G. Targher and G. Lippi, *Clin. Obstet. Gynecol.*, 2010, **53**, 219–227.
- 62 O. Warren, K. Mandal, V. Hadjianastassiou, L. Knowlton, S. Panesar, K. John, A. Darzi and T. Athanasiou, *Ann. Thorac. Surg.*, 2007, **83**, 707–714.
- 63 M. K. Klein, H. A. Kassam, R. H. Lee, W. Bergmeier, E. B. Peters, D. C. Gillis, B. R. Dandurand, J. R. Rouan, M. R. Karver, M. D. Struble, T. D. Clemons, L. C. Palmer, B. Gavitt, T. A. Pritts, N. D. Tsihlis, S. I. Stupp and M. R. Kibbe, *ACS Nano*, 2020, **14**, 6649–6662.
- 64 L. Lorand, *Ann. N. Y. Acad. Sci.*, 2001, **936**, 291–311.
- 65 A. Inbal, J. Oldenburg, M. Carcao, A. Rosholm, R. Tehranchi and D. Nugent, *Blood*, 2012, **119**, 5111–5117.
- 66 R. Hao, X. Peng, Y. Zhang, J. Chen, T. Wang, W. Wang, Y. Zhao, X. Fan, C. Chen and H. Xu, *ACS Appl. Mater. Interfaces*, 2020, **12**, 55574–55583.
- 67 B.-H. Hu and P. B. Messersmith, *J. Am. Chem. Soc.*, 2003, **125**, 14298–14299.
- 68 J. H. Collier and P. B. Messersmith, *Bioconjugate Chem.*, 2003, **14**, 748–755.
- 69 K. Ker, I. Roberts, H. Shakur and T. J. Coats, *Cochrane Database Syst. Rev.*, 2015, **5**, CD004896.
- 70 N. S. Gerstein, J. K. Brierley, J. Windsor, P. V. Panikkath, H. Ram, K. M. Gelfenbeyn, L. J. Jenkins, L. C. Nguyen and W. H. Gerstein, *J. Cardiothorac. Vasc. Anesth.*, 2017, **31**, 2183–2205.
- 71 L. Tengborn, M. Blomback and E. Berntorp, *Thromb. Res.*, 2015, **135**, 231–242.

- 72 A. Girish, D. A. Hickman, A. Banerjee, N. Luc, Y. Ma, K. Miyazawa, U. D. S. Sekhon, M. Sun, S. Huang and A. Sen Gupta, *J. Thromb. Haemost.*, 2019, **17**, 1632–1644.
- 73 P. Sasmal and P. Datta, *J. Drug Delivery Sci. Technol.*, 2019, **52**, 559–567.
- 74 D. Li, P. Li, J. Zang and J. Liu, *J. Biomed. Biotechnol.*, 2012, **2012**, 981321.
- 75 H. Su, S. Wei, F. Chen, R. Cui and C. Liu, *RSC Adv.*, 2019, **9**, 6245–6253.
- 76 U. Aydemir Sezer, Z. Kocer, B. Aru, G. Y. Demirel, M. Gulmez, A. Aktekin, S. Ozkara and S. Sezer, *RSC Adv.*, 2016, **6**, 95189–95198.
- 77 S. P. Myers, M. E. Kutcher, M. R. Rosengart, J. L. Sperry, A. B. Peitzman, J. B. Brown and M. D. Neal, *J. Trauma Acute Care Surg.*, 2019, **86**, 20–27.
- 78 A. Mahmoodzadeh, J. Moghaddas, S. Jarolmasjed, A. Ebrahimi Kalan, M. Edalati and R. Salehi, *Chem. Eng. J.*, 2021, **418**, 129252.
- 79 X. Zhao, B. Guo, H. Wu, Y. Liang and P. X. Ma, *Nat. Commun.*, 2018, **9**, 2784.
- 80 M. C. Gutiérrez, M. L. Ferrer and F. del Monte, *Chem. Mater.*, 2008, **20**, 634–648.
- 81 L. Wang, Y. Zhong, C. Qian, D. Yang, J. Nie and G. Ma, *Acta Biomater.*, 2020, **114**, 193–205.
- 82 J. F. Kragh, J. K. Aden, J. Steinbaugh, M. Bullard and M. A. Dubick, *Am. J. Emerg. Med.*, 2015, **33**, 974–976.
- 83 Y. Wang, Y. Zhao, L. Qiao, F. Zou, Y. Xie, Y. Zheng, Y. Chao, Y. Yang, W. He and S. Yang, *Bioact. Mater.*, 2021, **6**, 2089–2104.
- 84 S. Chen, M. A. Carlson, Y. S. Zhang, Y. Hu and J. Xie, *Biomaterials*, 2018, **179**, 46–59.
- 85 C. Wang, H. Niu, X. Ma, H. Hong, Y. Yuan and C. Liu, *ACS Appl. Mater. Interfaces*, 2019, **11**, 34595–34608.
- 86 X. Yang, M. Chen, P. Li, Z. Ji, M. Wang, Y. Feng and C. Shi, *J. Mater. Chem. B*, 2021, **9**, 1568–1582.
- 87 T. L. Landsman, T. Touchet, S. M. Hasan, C. Smith, B. Russell, J. Rivera, D. J. Maitland and E. Cosgriff-Hernandez, *Acta Biomater.*, 2017, **47**, 91–99.
- 88 X. Du, L. Wu, H. Yan, Z. Jiang, S. Li, W. Li, Y. Bai, H. Wang, Z. Cheng, D. Kong, L. Wang and M. Zhu, *Nat. Commun.*, 2021, **12**, 4733.
- 89 X. Zhao, Y. Liang, B. Guo, Z. Yin, D. Zhu and Y. Han, *Chem. Eng. J.*, 2021, **403**, 126329.
- 90 W. G. Malette, H. J. Quigley, R. D. Gaines, N. D. Johnson and W. G. Rainer, *Ann. Thorac. Surg.*, 1983, **36**, 55–58.
- 91 M. B. Dowling, R. Kumar, M. A. Keibler, J. R. Hess, G. V. Bochicchio and S. R. Raghavan, *Biomaterials*, 2011, **32**, 3351–3357.
- 92 J. Wen, M. Weinhart, B. Lai, J. Kizhakkedathu and D. E. Brooks, *Biomaterials*, 2016, **86**, 42–55.
- 93 G. Chen, Y. Yu, X. Wu, G. Wang, J. Ren and Y. Zhao, *Adv. Funct. Mater.*, 2018, **28**, 1801386.
- 94 N. Biezunski, E. Shafir, A. De Vries and E. Katchalski, *Biochem. J.*, 1955, **59**, 55–58.
- 95 H. Hattori and M. Ishihara, *Biomed. Mater.*, 2015, **10**, 015014.
- 96 X. Zhou, X. Zhang, J. Zhou and L. Li, *RSC Adv.*, 2017, **7**, 12247–12254.
- 97 Z. Hu, D. Y. Zhang, S. T. Lu, P. W. Li and S. D. Li, *Mar. Drugs*, 2018, **16**, 273.
- 98 K. Kim, J. H. Ryu, M.-Y. Koh, S. P. Yun, S. Kim, J. P. Park, C.-W. Jung, M. S. Lee, H.-I. Seo, J. H. Kim and H. Lee, *Sci. Adv.*, 2021, **7**, eabc9992.
- 99 S. Nam and D. Mooney, *Chem. Rev.*, 2021, **121**, 11336–11384.
- 100 C. Cui and W. Liu, *Prog. Polym. Sci.*, 2021, **116**, 101388.
- 101 Z. Ma, G. Bao and J. Li, *Adv. Mater.*, 2021, **33**, 2007663.
- 102 Y. Bu, L. Zhang, J. Liu, L. Zhang, T. Li, H. Shen, X. Wang, F. Yang, P. Tang and D. Wu, *ACS Appl. Mater. Interfaces*, 2016, **8**, 12674–12683.
- 103 M. A. Boerman, E. Roozen, M. J. Sanchez-Fernandez, A. R. Keereweer, R. P. Felix Lanao, J. Bender, R. Hoogenboom, S. C. Leeuwenburgh, J. A. Jansen, H. Van Goor and J. C. M. Van Hest, *Biomacromolecules*, 2017, **18**, 2529–2538.
- 104 Y. Bu, L. Zhang, G. Sun, F. Sun, J. Liu, F. Yang, P. Tang and D. Wu, *Adv. Mater.*, 2019, **31**, e1901580.
- 105 J. Li, A. D. Celiz, J. Yang, Q. Yang, I. Wamala, W. Whyte, B. R. Seo, N. V. Vasilyev, J. J. Vlassak and Z. Suo, *Science*, 2017, **357**, 378.
- 106 H. Yuk, J. Wu, T. L. Sarrafian, X. Mao, C. E. Varela, E. T. Roche, L. G. Griffiths, C. S. Nabzdyk and X. Zhao, *Nat. Biomed. Eng.*, 2021, **5**, 1131–1142.
- 107 C. K. Song, M.-K. Kim, J. Lee, E. Davaa, R. Baskaran and S.-G. Yang, *Macromol. Res.*, 2018, **27**, 119–125.
- 108 C. Liu, X. Liu, C. Liu, N. Wang, H. Chen, W. Yao, G. Sun, Q. Song and W. Qiao, *Biomaterials*, 2019, **205**, 23–37.
- 109 S. Zhang, J. Li, S. Chen, X. Zhang, J. Ma and J. He, *Carbohydr. Polym.*, 2020, **230**, 115585.
- 110 W. Huang, S. Cheng, X. Wang, Y. Zhang, L. Chen and L. Zhang, *Adv. Funct. Mater.*, 2021, **31**, 2009189.
- 111 K. A. Kristiansen, A. Potthast and B. E. Christensen, *Carbohydr. Res.*, 2010, **345**, 1264–1271.
- 112 Y. Hong, F. Zhou, Y. Hua, X. Zhang, C. Ni, D. Pan, Y. Zhang, D. Jiang, L. Yang, Q. Lin, Y. Zou, D. Yu, D. E. Arnot, X. Zou, L. Zhu, S. Zhang and H. Ouyang, *Nat. Commun.*, 2019, **10**, 2060.
- 113 J. H. Ryu, Y. Lee, W. H. Kong, T. G. Kim, T. G. Park and H. Lee, *Biomacromolecules*, 2011, **12**, 2653–2659.
- 114 C. Liu, W. Yao, M. Tian, J. Wei, Q. Song and W. Qiao, *Biomaterials*, 2018, **179**, 83–95.
- 115 S. Bai, X. Zhang, P. Cai, X. Huang, Y. Huang, R. Liu, M. Zhang, J. Song, X. Chen and H. Yang, *Nanoscale Horiz.*, 2019, **4**, 1333–1341.
- 116 X. Zhang, G.-h Sun, M.-p Tian, Y.-n Wang, C.-c Qu, X.-j Cheng, C. Feng and X.-g Chen, *Int. J. Biol. Macromol.*, 2019, **138**, 321–333.
- 117 Y. Shou, J. Zhang, S. Yan, P. Xia, P. Xu, G. Li, K. Zhang and J. Yin, *ACS Biomater. Sci. Eng.*, 2020, **6**, 3619–3629.
- 118 J. Sun, L. Xiao, B. Li, K. Zhao, Z. Wang, Y. Zhou, C. Ma, J. Li, H. Zhang, A. Herrmann and K. Liu, *Angew. Chem., Int. Ed.*, 2021, **60**, 23687–23694.
- 119 C. Cui, C. Fan, Y. Wu, M. Xiao, T. Wu, D. Zhang, X. Chen, B. Liu, Z. Xu and B. Qu, *Adv. Mater.*, 2019, **31**, 1905761.

- 120 L. Wang, X. Zhang, K. Yang, Y. V. Fu, T. Xu, S. Li, D. Zhang, L. N. Wang and C. S. Lee, *Adv. Funct. Mater.*, 2019, **30**, 1904156.
- 121 N. Holten-Andersen, M. J. Harrington, H. Birkedal, B. P. Lee, P. B. Messersmith, K. Y. Lee and J. H. Waite, *Proc. Natl. Acad. Sci. U. S. A.*, 2011, **108**, 2651–2655.
- 122 X. Xu, X. Xia, K. Zhang, A. Rai, Z. Li, P. Zhao, K. Wei, L. Zou, B. Yang, W.-K. Wong, P. W.-Y. Chiu and L. Bian, *Sci. Transl. Med.*, 2020, **12**, eaba8014.
- 123 X. Xia, X. Xu, B. Wang, D. Zhou, W. Zhang, X. Xie, H. Lai, J. Xue, A. Rai, Z. Li, X. Peng, P. Zhao, L. Bian and P. W. Y. Chiu, *Adv. Funct. Mater.*, 2021, 2109332.
- 124 J. J. Morrison, *Crit. Care Clin.*, 2017, **33**, 37–54.
- 125 R. I. Donaldson, E. M. Zimmermann, T. C. Fisher, O. J. Buchanan, J. K. Armstrong, J. S. Cambridge, T. L. Graham and J. D. Ross, *J. Surg. Res.*, 2021, **259**, 175–181.
- 126 H. T. Peng, *Mil. Med. Res.*, 2020, **7**, 13.
- 127 G. M. Taboada, K. Yang, M. J. N. Pereira, S. S. Liu, Y. Hu, J. M. Karp, N. Artzi and Y. Lee, *Nat. Rev. Mater.*, 2020, **5**, 310–329.
- 128 V. Tutwiler, J. Singh, R. I. Litvinov, J. L. Bassani, P. K. Purohit and J. W. Weisel, *Sci. Adv.*, 2020, **6**, eabc0496.
- 129 M. F. Cau, N. Ali-Mohamad, J. R. Baylis, V. Zenova, A. Khavari, N. Peng, A. McFadden, F. Donnellan, D. R. Owen, D. F. Schaeffer, C. Nagaswami, R. I. Litvinov, J. W. Weisel, J. Rezende-Neto, H. A. Semple, A. Beckett and C. J. Kastrup, *Injury*, 2022, **12**, DOI: [10.1016/j.injury.2022.01.024](https://doi.org/10.1016/j.injury.2022.01.024).
- 130 Y. Lu, Q. Hu, C. Jiang and Z. Gu, *Curr. Opin. Biotechnol.*, 2019, **58**, 81–91.
- 131 U. D. S. Sekhon and A. Sen Gupta, *ACS Biomater. Sci. Eng.*, 2018, **4**, 1176–1192.
- 132 T. Nitta, Y. Wang, Z. Du, K. Morishima and Y. Hiratsuka, *Nat. Mater.*, 2021, **20**, 1149–1155.